JHR 97: 441–470 (2024)
doi: 10.3897/jhr.97.118567
https://jhr.pensoft.net

RESEARCH ARTICLE

JOURNAL OF Hymenoptera RESEARCH
A peer-reviewed open-access journal
The International Society of Hymenopterists

Circumscription of the *Ganaspis brasiliensis* (Ihering, 1905) species complex (Hymenoptera, Figitidae), and the description of two new species parasitizing the spotted wing drosophila, *Drosophila suzukii* Matsumura, 1931 (Diptera, Drosophilidae)

Jeffrey Sosa-Calvo[1], Mattias Forshage[2], Matthew L. Buffington[3]

1 *Department of Entomology, Smithsonian NMNH, 10th and Constitution Ave NW, Washington DC 20013, USA* **2** *Naturhistoriska riksmuseet, Department of Zoology, Box 50007, SE-104 05 Stockholm, Sweden* **3** *Systematic Entomology Laboratory, USDA, c/o Smithsonian NMNH, 10th and Constitution Ave NW, Washington DC 20013, USA*

Corresponding authors: Jeffrey Sosa-Calvo (sossajef@si.edu); Matthew L. Buffington (matt.buffington@usda.gov)

Academic editor: Miles Zhang | Received 11 January 2024 | Accepted 11 April 2024 | Published 29 May 2024

https://zoobank.org/D7F62554-5C6E-4A64-98B2-628F2D94972B

Citation: Sosa-Calvo J, Forshage M, Buffington ML (2024) Circumscription of the *Ganaspis brasiliensis* (Ihering, 1905) species complex (Hymenoptera, Figitidae), and the description of two new species parasitizing the spotted wing drosophila, *Drosophila suzukii* Matsumura, 1931 (Diptera, Drosophilidae). Journal of Hymenoptera Research 97: 441–470. https://doi.org/10.3897/jhr.97.118567

Abstract

Based on host specificity and distribution data, it has been hypothesized that *Ganaspis brasiliensis* (Ihering, 1905), a natural enemy of the horticultural pest spotted-wing drosophila, *Drosophila suzukii* Matsumura, 1931 (SWD), was composed of multiple, cryptic species. Parasitoid wasps assigned to the species name *Ganaspis brasiliensis* and *Ganaspis* cf. *brasiliensis* were investigated using a molecular dataset of ultra-conserved elements (UCEs) and morphology. We report strong evidence for the presence of cryptic species based on the combination of UCE data (1,379 UCE loci), host specificity, ovipositor morphology, and distribution data. We describe these new cryptic species as: *Ganaspis lupini* **sp. nov.**, and *Ganaspis kimorum* **sp. nov.** *Ganaspis lupini* was formerly recognized as *Ganaspis brasiliensis* G3, and *Ganaspis kimorum* as *Ganaspis brasiliensis* G1. These two new species appear to be restricted to the temperate climates, whereas *Ganaspis brasiliensis* (formerly recognized as *Ganaspis brasiliensis* G5) has a more pan-tropical distribution. We investigated the characterization of the ovipositor clip of these species, and hypothesize that *G. kimorum*, which has a reduced ovipositor clip, has an advantage in ovipositing into fresh fruit, still on the host

plant, while attacking SWD; as a corollary, *G. brasiliensis* and *G. lupini*, which both have a larger ovipositor clip, are better adapted to attacking hosts in softer, rotting fruit on the ground. As *Ganaspis kimorum* was authorized for release as a biological control agent against SWD under the name *Ganaspis brasiliensis* G1, the results here have direct impact on the field of biological control.

Keywords
Biological control, cryptic species, pest fly, soft fruit, taxonomy

Introduction

Species that have not yet manifested morphological differences can often be separated based on molecular sequence data as well as behavioral data (Struck et al., 2018). These 'cryptic' species are a reality in modern systematics, and there are numerous examples recently published in Hymenoptera, including ants (Prebus 2021; Branstetter and Longino 2022; Schar et al. 2022), encyrtid wasps (Wang et al. 2016), eulophid wasps (Hansson and Hamback 2013), aphelinid wasps (Heraty et al. 2007), microgastrine braconids (Alex Smith et al. 2013) and parasitoids of cynipid wasps (Zhang et al. 2022), to mention some. Within biological control research, cryptic species can present a major challenge in finding the safest, most reliable, natural enemy (Rosen 1986).

Ganaspis brasiliensis (Ihering, 1905) (Hymenoptera: Figitidae: Eucoilinae) has been hypothesized to be a cryptic species complex (Nomano et al. 2017; Hopper et al. 2024). While a great deal of international exploration has been conducted in pursuit of natural enemies of the spotted-wing drosophila (SWD), *Drosophila suzukii* Matsumura, 1931 (Diptera: Drosophilidae) (Nomano et al. 2017; Giorgino et al. 2018; Abram et al. 2022), much work has also been conducted on which wasp populations attack this pest with the most specificity. *Ganaspis brasiliensis* was, early on, recognized as a common natural enemy of SWD, and was redescribed (Buffington and Forshage 2016). Since then, additional field and lab studies (summarized by Seehausen et al. 2020) have suggested *G. brasiliensis* could in fact be a cryptic species complex, composed of as many as five species (Nomano et al. 2017). The study by Nomano et al (2017) reported five lineages of *G. brasiliensis*, namely G1–G5. Since that study, G1 has been recognized as the most host-specific population of *G. brasiliensis* (Giorgini et al. 2018; Abram et al. 2022) and has even been cleared for release in the United States by USDA-APHIS; G3, also a natural enemy of SWD, has a slightly broader host range, and where it co-occurs with G1, a slightly less effective natural enemy of SWD; and G5 appears to be pan-tropical and not able to exploit SWD at all; other *Drosophila* species are hosts for G2 and G4 (Nomano et al. 2017). Altogether, these data led Seehausen et al. (2020) to set the stage for these populations of *G. brasiliensis* G1, G3, and G5, to be recognized as distinct species (G2 and G4 lacked sufficient sample data). Hopper et al. (2024) presented whole genome datasets that suggest G1 and G3 are in fact separate species (although G5 was not included, as it has not been recorded attacking SWD).

We utilize an integrative approach, including novel ultra-conserved element (UCE) molecular data, morphological data (based on ovipositor and scutellar characters), published host specificity studies, published crossing experiments, and distribution data to distinguish at least three lineages within the formerly recognized *Ganaspis brasiliensis*. As such, we herewith describe two new species: *Ganaspis kimorum*, new species, and *Ganaspis lupini*, new species. In light of these new data, *Ganaspis brasiliensis* is redescribed and the circumscription of this species updated.

Materials and methods

Specimen acquisition

The source for all specimens in this study resulted from the combined rearing efforts of collaborators from around the world, as well as researchers with established *Ganaspis* spp. laboratory colonies for genetic research; these collaborators are listed in Suppl. material 1: table S1 as well as in the acknowledgments. As specimens were reared in the field or the lab, a subset of specimens was sent to one of us (MLB) for morphological determination and vouchering in the National Museum of Natural History, Smithsonian Institution (USNM); these were typically dry mounted and labeled, but some were retained in 95% ethanol. In some cases, large numbers of specimens were sent and kept in 95% ethanol. Outgroups included were *Ganaspis hookeri* (Crawford, 1913) (from a laboratory colony), two other undescribed, but morphologically distinct, species of *Ganaspis*, that were bred true from a laboratory colony, and specimens identified as belonging to the eucoiline genus *Leptopilina* Föster.

Specimen illustration and observation

Representative specimens were imaged using the Macropod®™ multiple-focus imaging system to illustrate diagnostic characters; single montage images were produced from image stacks with the program Zerene Stacker®™. Scanning electron micrographs were generated using a Hitachi®™ TM3000 desktop scanning electron microscope; specimens were coated in 25–30 nm gold-palladium alloy (Cressington®™ 108 auto sputtercoater), using 'analysis' voltage, running in 'compo' mode. Diagnoses focus on easily recognized gross morphologies, and species/genera that can be confused with *G. brasiliensis* are diagnosed. Terminology for all descriptive characters, as well as phylogenetic characters, follow Buffington and Forshage (2016).

DNA extraction

DNA was extracted using the Qiagen DNeasy® Blood and Tissue Kit (Qiagen, Valencia, CA, U.S.A.). DNA extractions were performed by either placing an entire individual (male or female) or their metasoma, in a 2 mL tube with 0.5 mm diameter glass

lysis beads (BioSpec Products, Bartlesville, OK, U.S.A.). The samples were placed in a -20 °C freezer for ~10 minutes and then placed in a TissueLyser II (Qiagen Inc., USA) for 30 s at 30 Hz to disrupt the tissue and facilitate the lysis process. Cell lysis was performed overnight with 20 µL of Proteinase K in a dry bath shaker at 56 °C and at 500 rpm. The recommendations of the manufacturer were followed for the extraction process except that the cleaned, extracted DNA from the spin-collection columns was eluted with two (rather than one) washes, each consisting of 55 µL of nuclease-free water, differing from the manufacturer's recommendation of 200 µL of AE buffer. DNA extractions were quantified using 2 µL of DNA template in a Qubit 4 Fluorometer and with the 1X dsDNA High Sensitivity (HS) assay Kit (Thermo Fisher Scientific, Inc.). DNA extraction concentration ranged from 0.001–7.20 ng/µL (mean = 0.943 ng/µL).

Generation of UCE data: Library preparation

Prior to library preparation, 1–50 ng of DNA template was sheared to an average fragment length of 300–600 bp using a Qsonica Q800R2 Sonicator (Qsonica LLC, Newton, CT, U.S.A.) for 60 s with amplitude set at 25 and the pulse set at 10. Libraries were prepared on 96-well plates on a DynaMag™-96 side magnet (Invitrogen, Thermo Fischer Scientific, Waltham, MA, U.S.A.) and using the Kapa Hyper Prep Library Kit (Roche Diagnostics Corporation, Indianapolis, IN, U.S.A.) as described in Faircloth et al. (2015) with the iTru Adapter protocol. We implemented all magnetic bead clean-up steps (Fisher et al. 2011) as described in Faircloth et al. (2015) and used dual-indexing TruSeq adapters (Faircloth and Glenn 2012, Glenn et al. 2019) for ligation. The ligation step was followed by PCR-amplification of 15 µL of the library product using 25 µL of KAPA HiFi ReadyMix (Roche Diagnostics Corporation, Indianapolis, IN, U.S.A.), 2.5 µL of each of Illumina TruSeq (i5 and i7) primers, and 5 µL nuclease-free ddH_2O. The following thermal cycler program was executed: 98 °C for 45 s; 13 cycles of 98 °C for 15 s, 60 °C for 30 s, 72 °C for 60 s; and final extension at 72 °C for 5 m. Following PCR, we purified DNA products using 1.1× Kapa Pure beads and rehydrated the purified product in 22 µL of Elution Buffer (pH = 8). Individual libraries were quantified using 2 µL of library product in a Qubit 4 Fluorometer using the 1X dsDNA Broad Range (BR) assay Kit (Thermo Fisher Scientific, Inc.). Post-PCR libraries have concentrations ranging from 3.05–114.9 ng/µL.

Library pooling and target enrichment of libraries

Post-PCR libraries were pooled at equimolar concentrations into 25 pools, each containing 6–12 libraries. Pool concentration was adjusted to ~71.5 ng/µL by drying the sample in a vacuum centrifuge for 45–60 min or until all liquid was evaporated at 60 °C, and then by re-suspending the pool in nuclease-free water at the estimated volume. We then used 2 µL of the resuspended product to measure the pool final concentration in a Qubit 4 Fluorometer with the 1X dsDNA BR assay Kit. The final concentration of the pre-enrichment pools was 63.6–91.4 ng/µL. The pool was enriched by

using the myBaits (Arbor Biosciences, Ann Harbor, MI, U.S.A.) UCE Hymenoptera bait set ("Hymenoptera 2.5Kv2P") targeting 2590 conserved loci in Hymenoptera (Branstetter et al. 2017) at an incubation temperature of 65 °C for 24 h in a thermal cycler. Enrichment, bead-cleaning, and PCR reaction procedures partially followed the Arbor Biosciences v5.0.1 (https://arborbiosci.com/mybaits-manual/) protocol and Branstetter et al. (2021) and Hanisch et al. (2022). The resulting reaction was purified using 1.0X Kapa Pure beads (Roche Diagnostics Corporation, Indianapolis, IN, U.S.A.) and the enriched pool was then rehydrated in 22 µL elution buffer. The final two enriched pools were submitted to Admera Health Biopharma Services (NJ, U.S.A.) for quality control and sequencing of two lanes on an Illumina HiSeq2500 instrument. A summary of the raw data, contigs, UCE loci recovered, and other assembly statistics for each sample is presented in Suppl. material 1: table S2. Most extractions and UCE laboratory work were conducted in the Laboratories of Analytical Biology (LAB) facilities of the National Museum of Natural History, Smithsonian Institution. New raw sequences generated as part of this study are deposited in the NCBI Sequence Read Archive (SRA) under BioProject number PRJNA1088885 and under accession No. SAMN40504884–SAMN40505120.

Molecular phylogenetics: Processing of UCE sequence data

We trimmed the demultiplexed FASTQ output files for adapter contamination and low-quality bases using Illumiprocessor v.2.0.6 (Faircloth 2013, modified by R. Dikow and P. Frandsen to use trim_galore v0.4.1 (Krueger 2015)). We used SPAdes v.3.14 (Bankvich et al. 2012, Nurk et al. 2013) to assemble the clean reads into contigs. We used a series of scripts available in the PHYLUCE package (Faircloth 2016) to further process our data and we followed the methods used in Barrera et al. (2022), Hanisch et al. (2022), Blaimer et al. (2023). We aligned each UCE locus using MAFFT v7.407 (Katoh and Standley 2013) using the default algorithm. The alignment step was repeated using the L-INS-I algorithm in MAFFT, which tends to generate more accurate alignments (Katoh et al. 2005, Katoh and Standley 2014). We trimmed poorly aligned regions in each UCE locus with GBLOCKS (Castresana 2000, Talavera and Castresana 2007) using relaxed settings (b1 = 0.5, b2 = 0.5, b3 = 12, b4 = 7). Initial alignments were generated by first aligning individual UCE loci with different percentage of taxon representation, thus 50% (119 taxa, 1,477 loci), 60% (143 taxa, 1,379 loci) and 70% (166 taxa, 1,211 loci) using the PHYLUCE script *phyluce_align_get_only_loci_with_min_taxa*. We then concatenated those loci into a data matrix using the PHYLUCE script *phyluce_align_format_nexus_files_for_raxml*, named Ganasbra237t_50p, Ganasbra237t_60p, and Ganasbra237t_70p, respectively, for exploratory and downstream analyses.

UCE phylogenetic analyses

Initial analyses were conducted on the unpartitioned three alignments generated (Ganasbra237t at 50%, 60%, and 70%, respectively) using IQ-TREE multicore v.2.1.3

(Minh et al. 2020), the GTR+F+G4 model of evolution (as selected by IQ-TREE), the default number of unsuccessful iterations to stop (-nstop 100), and an initial neighbor-joining tree (-t BIONJ). Node support was estimated by conducting 1,000 ultrafast bootstraps (UFBoot) (Hoang et al. 2018).

To identify and remove outlier or poorly aligned sequence fragments we used the Python tool SPRUCEUP (Borowiec 2019) on the Ganasbra237t_60p alignment. Parameters in the configuration file were set up to the uncorrected p-distance for computing the distances, window size = 20 bp and overlap = 15 bp, a lognormal distribution to identify outlier distances, and a global cutoff of 0.997. As a result, SPRUCEUP removed 56,045 (0.02%) outlier nucleotide-site state assignments (i.e., matrix cell values (Suppl. material 1: table S3). We then used the resulting SPRUCEUP-trimmed alignment and repeated the unpartitioned analysis using the same parameters as above, including 1,000 replicates of the SH-like approximation likelihood-ratio test (-alrt 1000) (Guindon et al. 2010). Upon inspection of the resulting tree and the png files generated by SPRUCEUP, additional, manual cutoffs were performed for 23 taxa (see Suppl. material 1: table S3 for cutoff values).

We partitioned the resulting trimmed alignment using the Sliding Window Site Characteristics based in Entropy method (SWSC-EN; Tagliacollo and Lanfear 2018), in which each UCE locus is divided into three regions (a core and two flanking regions). The SWSC-EN algorithm identified 4,137 subsets. We then identified the best partitioning scheme by merging the resulting subsets using ModelFinder (Kalyaanamoorthy et al. 2017) as implemented in IQ-TREE (Minh et al. 2020). For the merging step, we used the *-m MF+MERGE* command, the fast relaxed *-rclusterf* algorithm (set to 10; Lanfear et al. 2017) and compared the top 10% of the resulting partitioning schemes using the corrected Akaike information criterion (AICc), restricting the evaluated models to those implemented in RAxML by using the command *-mset raxml*. The best-fit partitioning scheme (0.997_lognorm_man_Ganasbra237t_60p_SWSCEN) consisted of 1,629 partitions.

We tested for model violation based on assumptions of stationarity and homogeneity by performing a test of symmetry (Naser-Khdour et al. 2019) as implemented in IQ-TREE 2.1.3 (Chernomor et al. 2016; Minh et al. 2020) on the partitioned dataset above. We removed bad partitions by using the *–symtest-remove-bad* option with a *P*-value cutoff set as the default ($P = 0.05$). The test of symmetry identified and removed 536 out of the 4,137 subsets generated by SWSC-EN. The resulting best-fit partitioning scheme (0.997_lognorms_cutoff_man_Ganaspis237-60p_partitions.nex.good_SYMTEST) consisted of 1,422 partitions.

We performed further maximum-likelihood (ML) analyses on the trimmed alignment with the different partitioning schemes using IQ-TREE multicore v.2.1.3 (Chernomor et al. 2016; Minh et al. 2020), estimating branch support with the ultrafast bootstrap (Hoang et al. 2018) and the SH-like approximation likelihood ratio test (Guindon et al. 2010) set at 1,000 replicates, with other settings set at default values on the 0.997_lognorms_cutoff_man_Ganaspis237-60p_partitions.nex.good_SYMTEST alignment. Statistics for all the data matrices generated for this study are summarized

in Suppl. material 1: table S4 and all trees generated for this study are in supplementary information (https://figshare.com/s/93d692506c0fe68a7ddd).

We employed the *species delimitation* plugin v.1.4.5 (Masters et al. 2011) in Geneious Prime (www.biomatters.com) to summarize the average pairwise tree distance (using the tree in Fig. 6) among members of a clade (Intra Dist) and the average pairwise tree distance among a clade and its closest clade (Inter Dist). Results are summarized in Table 1 and Suppl. material 1: table S5.

Generation of DNA Barcoding (COI)

Employing the Phyluce script *phyluce_assembly_match_contigs_to_barcode* and a COI sequence as reference ('*Ganaspis brasiliensis*' downloaded from GenBank accession No. MN013168.1), we extracted from the UCE data bycatch (Ströher et al. 2017) the *cytochrome oxidase I* (COI) gene fragment for a subset of samples, including from a non-type specimen of the original description of *Ganaspis brasiliensis* not included in the UCE data analyses above. The *contig.slice* files were then inspected in Geneious Prime v.2024.0.4 (www.biomatters.com) and mapped to the reference sequence (MN013168.1) using the BBMap v.1.0 (Bushnell 2014) plugin. COI sequences, of some specimens, are given at the end of the description of each species, and they have also been deposited in GenBank under accession No. PP599368–PP599375 (see Suppl. material 1: table S6).

Results

UCE sequencing and matrix assembly

In average, we recovered 1,369 UCE loci (range: 672–1,670) with a mean length of 878 bp (range: 341–1,801 bp). The final alignment included 237 terminals, 1,379 UCE loci, and 1,221,982 bp of sequence data, of which 523,179 were parsimony-informative sites. The alignment was composed mostly of samples in the genus *Ganaspis* and two samples belonging to the genus *Leptopilina* Föster, 1862, as a distant outgroup. The test of symmetry conducted in IQTREE 2.1.3 (Chernomor et al. 2016; Minh et al. 2020) identified and removed 536 and 565 bad partitions depending on the SPRUCEUP manual cut-off employed (Suppl. material 1: table S3). The resulting 'good' alignments consisted of 964,889 and 960,213 bp of sequence data and 427,640 and 427,499, respectively. For additional assembly and additional statistics, see Suppl. material 1: table S4. All trees generated in this study are deposited in supplemental information (https://figshare.com/s/93d692506c0fe68a7ddd).

Morphological study

Morphological examination of the scutellum and ovipositor revealed subtle but consistent differences among specimens examined (Fig. 3). For the scutellum, the lateral

Table 1. Summary of differences among species in the *Ganaspis brasiliensis* species complex.

Species	Host	Distribution	scutellum	Ovipositor clip	Intra-species genetic distance	Inter species genetic distance
Ganaspis brasiliensis	*D. melanogaster* *D. simulans* other *Drosophila*	Pan tropical: Neotropical, Afrotropical, Hawaiian	sides with carinae/ grooves	Present, large	0.041	0.076
Ganaspis lupini	SWD and other *Drosophila*	Palearctic: China, Japan, Korea	sides smooth	Present, large	0.05	0.067
Ganaspis kimorum	SWD	Palearctic: China, Japan, Korea, Nearctic: USA, Canada	sides smooth	Present, small to indistinguishable	0.021	0.075

aspects were carinate/striate in tropical specimens (*G. brasiliensis*), but totally smooth in more temperate specimens (*G. kimorum*, *G. lupini*). Further, members of *G. kimorum* were discovered to have a reduced ovipositor clip (Fig. 4). Research on the genome (Hopper et al. 2024), host specificity (Girod et al. 2018b; Wang et al. 2018; Seehausen et al. 2020; Daane et al. 2021), reproductive isolation (Seehausen et al. 2020; Hopper et al. 2024), and DNA barcode region (Nomano et al. 2017) are consistent with the morphological characters and UCE phylogenomic data shown here (Fig. 6). Together these data support the description of *G. kimorum* and *G. lupini* as species new to science. Fig. 6 shows the phylogram of these species; major sources of specimens are highlighted. Table 1 summarizes the various lines of study for species delimitation.

Ganaspis brasiliensis species group

Included species. *Ganaspis brasiliensis* (Ihering, 1905); *Ganaspis kimorum* sp. nov.; *Ganaspis lupini* sp. nov.

Diagnosis. Scutellum large, terminating anterior to the end of the scutellum; convex in lateral view, bulging slightly. Marginal cell closed in forewing. Posterior edge of metapleuron uninterrupted. Segments of female antennal clava very moderately enlarged and concolorous with other flagellomeres (Buffington and Forshage 2016). In the *Ganaspis brasiliensis* species group, the plate covers at least half of the scutellum, when viewed dorsally; in lateral view, the scutellar plate is clearly convex, even bulging, anterior to the glandular release pit. In other *Ganaspis* species, the scutellar plate may be as large or smaller, covering less than half of the scutellum when viewed dorsally; the plate, in lateral view, is flat or gently convex, and if large, not bulging. The marginal cell and claval characters are quite variable in other *Ganaspis* species.

Description. Coloration with head, mesosoma, and metasoma black to dark brown; legs uniformly light brown. Sculpture on vertex, lateral surface of pronotum, mesosoma, and metasoma absent, surface entirely smooth (Fig. 1). Length 1.5–1.75 mm.

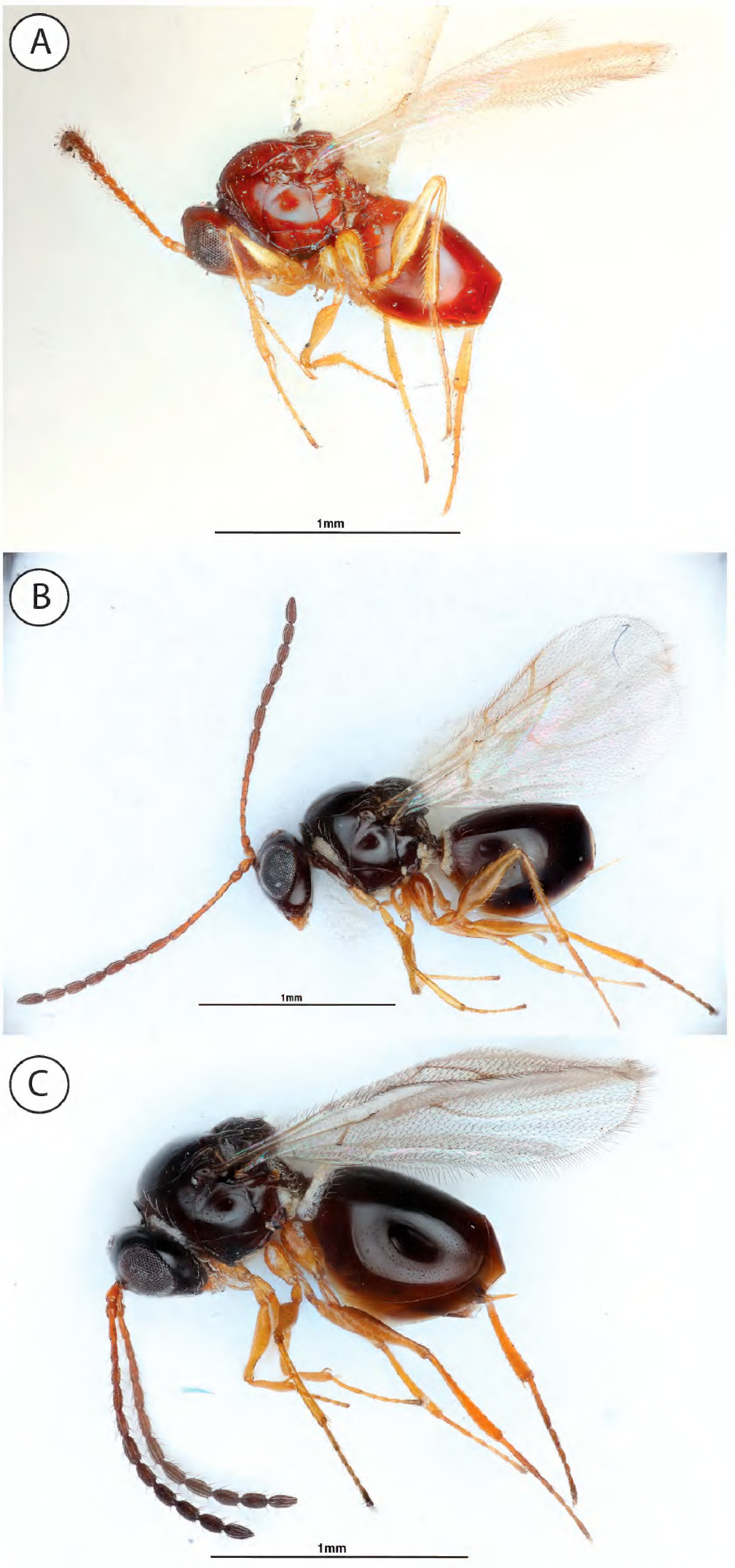

Figure 1. Type-specimens of the species belonging to the *G. brasiliensis* species complex **A** *brasiliensis*, lectotype **B** *kimorum*, holotype **C** *lupini*, holotype.

Head. In anterior view, rounded, approximately as high as broad; in lateral view, more transverse, not protruding. Pubescence on head sparse, nearly glabrous. Sculpture along lateral margin of occiput absent (Fig. 2A). Gena (measured from compound eye to posterolateral margin of head) short, ratio of length of gena to length of compound eye in dorsal view <0.3 mm. Sculpture of gena absent, smooth. Lateral margin of occiput evenly rounded, not well defined (Fig. 2A). Occiput (except extreme lateral margin) smooth. Carina issuing from lateral margin of postocciput absent. Ocelli small, ratio of maximum diameter of a lateral ocellus to shortest distance between lateral ocelli 0.2–0.4 mm. Anterior ocellus far from posterior ocelli, clearly anterior to anterior margins of posterior ocelli. Relative position of antennal sockets close to ocelli, ratio of vertical distance between inner margin of antennal foramen and ventral margin of clypeus to vertical distance between anterior ocellus and antennal rim <2.0. Median keel of face absent. Vertical carina adjacent to ventral margin of antennal socket absent. Facial sculpture absent, surface smooth. Facial impression absent, face flat. Antennal scrobe absent. Anterior tentorial pits small. Longitudinal axis of posterior tentorial pits oblique. Vertical delineations on lower face absent. Ventral clypeal margin laterally, close to anterior mandibular articulation, straight. Ventral clypeal margin medially straight, not projecting. Clypeus smooth, evenly rounded. Malar space adjacent to anterior articulation of mandible evenly rounded, smooth. Malar sulcus present. Eye close to ocelli, ratio of distance between compound eye and posterior mandibular articulation to distance between posterior ocellus and compound eye >1.2 mm. Compound eyes, in dorsal view, distinctly protruding from the surface of the head, particularly laterally. Pubescence on compound eyes absent. Orbital furrows absent. Lateral frontal carina of face absent. Dorsal aspect of vertex smooth. Posterior aspect of vertex smooth. Hair punctures on lateral aspect of vertex absent. Posterior surface of head deeply impressed around post-occiput.

Labial-maxillary complex. Apical segment of maxillary palp with pubescence, consisting only of erect setae. First segment of labial palp shorter than apical segment. Labial palp composed of two segments. Apical seta on apical segment of maxillary palp longer than twice length of second longest apical seta. Erect setae medially on apical segment of maxillary palp absent. Maxillary palp composed of four segments. Last two segments of maxillary palp (in normal repose) curved inwards. Distal margin of subapical segment of maxillary palp slanting inwards, apical segment bending inwards. Apical segment of maxillary palp more than 1.5× as long as preceding segment.

Antenna. Articulation between flagellomeres in antenna moniliform, segments distinctly separated by narrow neck-like articulation (Fig. 2C). Female antenna composed of 11 flagellomeres (Fig. 2C). Male antenna composed of 13 flagellomeres. Female F1 longer than F2. Flagellomeres of female antenna cylindrical, gently widened towards apex, slightly clavate (Fig. 2C). Placoidal sensilla present on F6-11 (Fig. 2C). Second flagellomere of male antenna cylindrical. Length of second flagellomere of male antenna equal to length of first flagellomere. Last antennal flagellomeres of female antenna not conspicuously enlarged compared to adjacent flagellomeres (Fig. 2C).

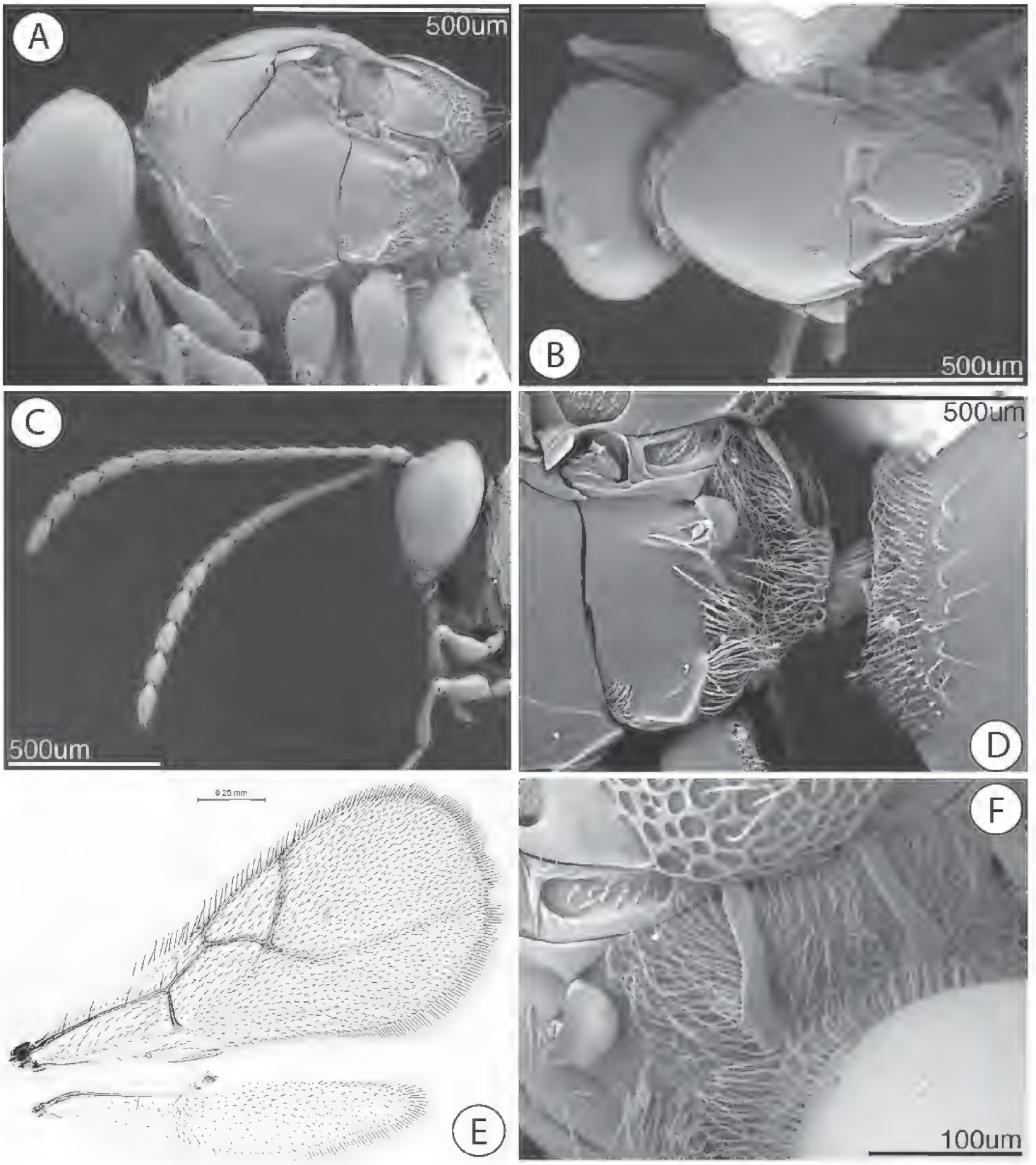

Figure 2. External anatomy of *Ganaspis kimorum*, a member of the *Ganaspis brasiliensis* species complex **A** head and mesosoma, lateral view **B** head and mesosoma, dorsal view **C** femal antennae **D** metapectal-propodeal complex, lateral view **E** fore- and hindwings, female **F** propodeum, dorso-lateral view.

Mesosoma. Macrosculpture on lateral surface of pronotum absent (Fig. 2A). Anteroventral inflection of pronotum narrow. Pubescence on lateral surface of pronotum present, sparse, consisting of few short hairs posterior to setal trench (Fig. 2A). Anterior flange of pronotal plate subvertical, protruding, transversely strigate. Ridges extending posteriorly from lateral margin of pronotal plate absent (Fig. 2A). Lateral pronotal carina absent. Crest of pronotal plate absent. Dorsal margin of pronotal plate (in anterior

view) straight; rounded. Submedian pronotal depressions open laterally, deep. Lateral margin of pronotal plate defined all the way to the dorsal margin of the pronotum. Width of pronotal plate narrow, not nearly as wide as head (Fig. 2B). Mesoscutal surface convex, evenly curved (Fig. 2A). Sculpture on mesoscutum absent, entire surface smooth, shiny (Fig. 2B). Notauli absent. Median mesoscutal carina absent. Anterior admedial lines absent. Median mesoscutal impression absent. Parascutal carina nearly straight anteriorly, posteriorly curved mesally. Mesopleuron entirely smooth (Fig. 2A). Subpleuron entirely smooth, glabrous (Fig. 2A). Lower pleuron entirely smooth, glabrous. Epicnemial carina absent. Lateroventral mesopleural carina present, marking abrupt change of slope of mesopectus (Fig. 2A). Mesopleural triangle present, slightly impressed without distinct ventral border (Fig. 2A). Subalar pit absent, subalar groove indistinct. Speculum absent. Mesopleural carina present, complete, composed of one complete, uninterrupted carina (Fig. 2A). Anterior end of mesopleural carina inserting above notch in anterior margin of mesopleuron. Dorsal surface of scutellum foveate-areolate (Figs 2B, 3). Circumscutellar carina absent (Fig. 3). Posterior margin of axillula marked by distinct ledge, axillula distinctly impressed adjacent to ledge (Fig. 3 A, C, E). Latero-ventral margin of scutellum posterior to auricula entirely smooth (Fig. 3A, C, E). Dorsoposterior part of scutellum rounded (Fig. 3A, C, E). Transverse median carina on scutellar plate absent. Dorsal part of scutellum entirely foveate. Scutellar plate large, widest in anterior half, covering most of scutellum; dorsally smooth, polished; glandular release pit at posterior end (Fig. 3B, D, F); in lateral view, often with an anterior hump, sunken around release pit, slightly upturned along posterior margin (Fig. 3A, C, E). Scutellar fovea present, two, distinctly margined posteriorly (Fig. 3B, D, F). Single longitudinal carina separating scutellar foveae present, short, ending at posterior margin of foveae (Fig. 3B, D, F). Longitudinal scutellar carinae absent. Postero-lateral margin of scutellum rounded. Lateral bar weakly strigate, narrow.

Metapectal-propodeal complex. Metapectal cavity anterodorsal to metacoxal base present, well-defined (Fig. 2D). Anterior margin of metapectal-propodeal complex meeting mesopleuron at same level at point corresponding to anterior end of metapleural carina. Posteroventral corner of metapleuron (in lateral view) rounded, not drawn out posteriorly (Fig. 2D). Anterior impression of metepimeron absent. Posterior margin of metepimeron distinct, with median part slightly depressed, not forming circular incision, separating metepimeron from propodeum (Fig. 2D). Subalar area slightly broadened anteriorly, with distinct laterally protruding lobe ventrally. Prespiracular process present, blunt, lobe-like, polished (Fig. 2D). Dorsellum present, smooth, glabrous. Anterior impression of metepisternum, immediately beneath anterior end of metapleural carina, absent. Pubescence not extremely dense on posterior part of metapectal-propodeal complex (Fig. 2D). Propodeal spurs absent (Fig. 2D). Lateral propodeal carinae present, elongate, projecting beyond metanotum to reach scutellum (Fig. 2D). Ventral end of lateral propodeal carina reaching nucha, carinae separated from each other. Inter propodeal carinae space lightly setose, smooth. Petiolar rim of uniform width along entire circumference. Petiolar foramen removed from metacoxae, directed posteriorly. Horizontal carina running anteriorly from lateral propodeal carina

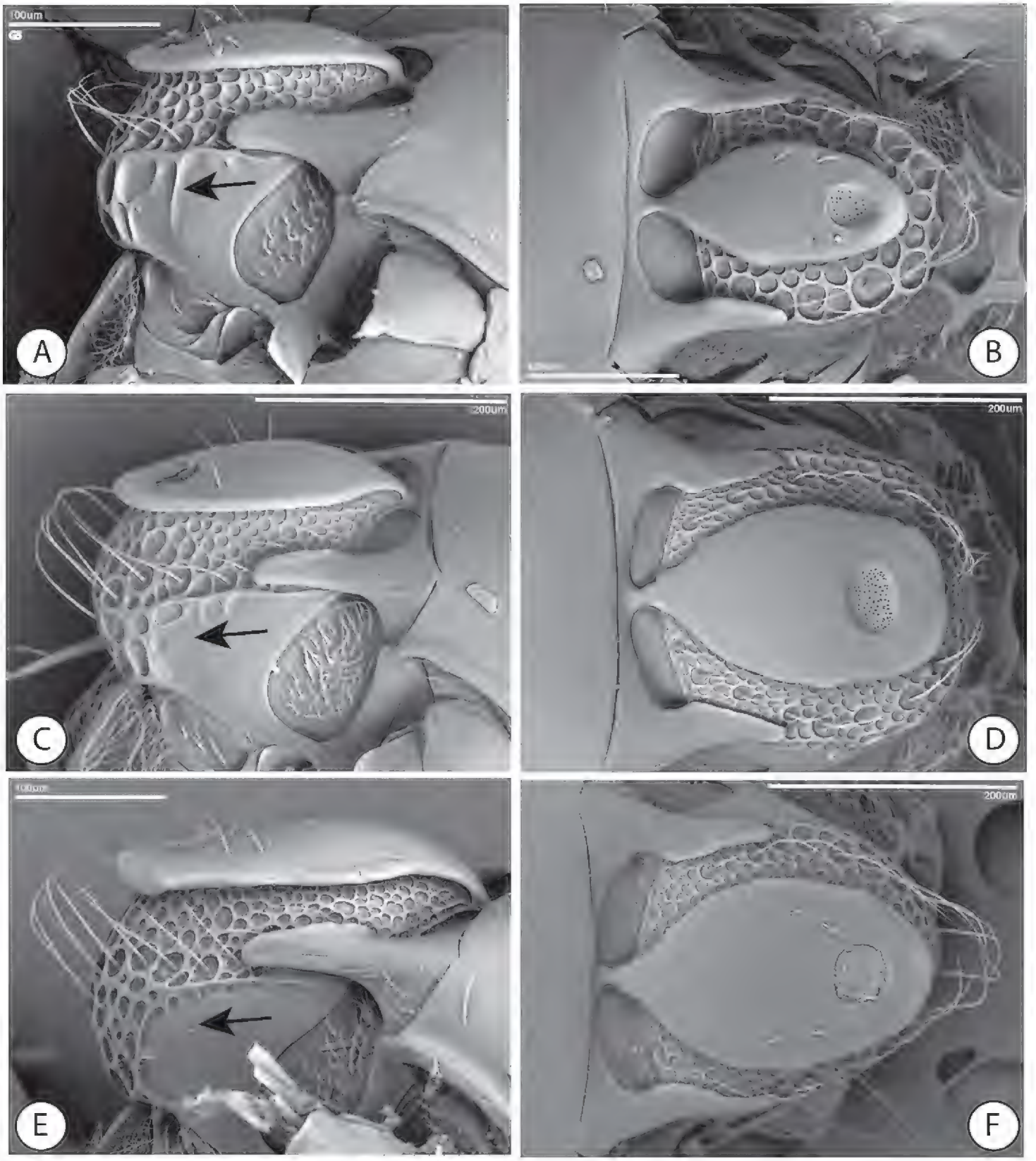

Figure 3. Comparison of the scutellar morphology between *G. brasiliensis* (**A, B**), *G. lupini* (**C, D**) and *G. kimorum* (**E, F**). Black arrows indicate sculptured (**A**) and smooth (**C, E**) lateral aspect of scutellum.

present. Lateral propodeal carina uniformly curved inward. Calyptra, in lateral view, rounded. Propodeum relatively short, not drawn out posteriorly (Fig. 2D). Calyptra, in posterior view, rounded.

Legs. Pubescence posterolaterally on metacoxa with a confined, elongate, dense hair patch, other pubescence lacking. Microsculpture on hind coxa absent (Fig. 2A). Longitudinal ridge on the posterior surface of metatibia absent. Metafemoral tooth absent. Distal mesotibial spurs shorter than medial spurs. Distal metatibial spurs shorter than medial spurs. Ratio of first metatarsal segment to remaining 4 segments <1.0.

Pubescence on outer surface of metatarsal claw sparse, consisting of few setae. Outer surface of metatarsal claw almost entirely smooth. Base of metatarsal claw lammelate, with translucent cuticular flange.

Wings. Pubescence of fore wing present, long, dense on most of surface (Fig. 2E). Apical margin of female fore wing rounded. Rs+M of forewing completely defined (Fig. 2E). Vein R1 tubular along at least basal part of anterior margin of marginal cell. Mesal end of Rs+M vein situated closer to posterior margin of wing, directed towards posterior end of basalis (Fig. 2E). Basal abscissa of R1 (the abscissa between 2r and the wing margin) of fore wing as broad as adjacent wing veins. Coloration of wing absent, entire wing hyaline (Fig. 2E). Marginal cell of fore wing membranous. Areolet absent. Hair fringe along apical margin of fore wing present, very short.

Metasoma. Petiole about as long as wide. Surface of petiole dorsally striate, laterally shagreen. Posterior part of female petiole not abruptly widened. Ventral flange of annulus of female petiole absent. Ventral and lateral parts of petiolar rim narrow. Setal band (hairy ring) at base of tergum 3 present, complete dorsally, extending ventrally to ventral margin of tergum, beneath petiole. Tergum 3 indistinct, fused with syntergum. Posterior margin of tergum 3 indistinct, fused with tergum 4 in syntergum. Posterior margin of tergum 4 evenly rounded. Sternum 3 encompassed by syntergum. Sculpture on metasomal terga absent. Syntergum present with terga 3 to 5 fused, ventral margin rounded. Annulus present as continuous ring. Peglike setae on T6–T7 absent. Postero-ventral cavities of female metasoma T7 absent. Female postero-ventral margin of T6–T7 straight, parallel, with distinct postero-ventral setal tuft. Terebrum and hypopygium (in lateral view) straight, pointing posteriorly. Ovipositor clip present.

Ganaspis brasiliensis (Ihering, 1905)

Figs 1A, 3A, B, 4A

Diagnosis. Separated from *G. kimorum* and *G. lupini* by the sculpturing on the side of the scutellum. In *G. brasiliensis*, this area has distinct dorso-ventral carinae enclosing one or a few cells (Fig. 3A). In *G. kimorum* and *G. lupini*, this area is totally smooth (arrows, Fig. 3C, E). Further separated from *G. kimorum* by the well-developed ovipositor clip that is expanded across more the half the width of the ovipositor valve (Fig. 4A).

Redescription. As in the description for the *G. brasiliensis* species complex, but lateral aspect of pronotum with distinct ridge with associated fovea; ovipositor clip large, extending beyond the halfway point across the fused ovipositor valve. Previous studies referencing 'Gb G5' or 'G5', refer to this species (Nomano et al. 2017).

Material examined. Lectotype (female): Collection Ashmead [first label]; Ipiranga, Brazil [second label]; No 2066 from a peach [third label]; S.S. Paulo Museum 190 [third label]; Lectotype [fourth label, red, Weld's hand]; Ipiranga, S.S. Paulo Museum 190, No. 4066a, on peach [folded hand-written label]; EUCOILIDAE, *Pseudeucoila* (*Hexamerocera*) *brasiliensis* Ashmead [white computer generated label]; USNMENT0119750. Deposited in USNM. Paralectotype (male): Collection Ash-

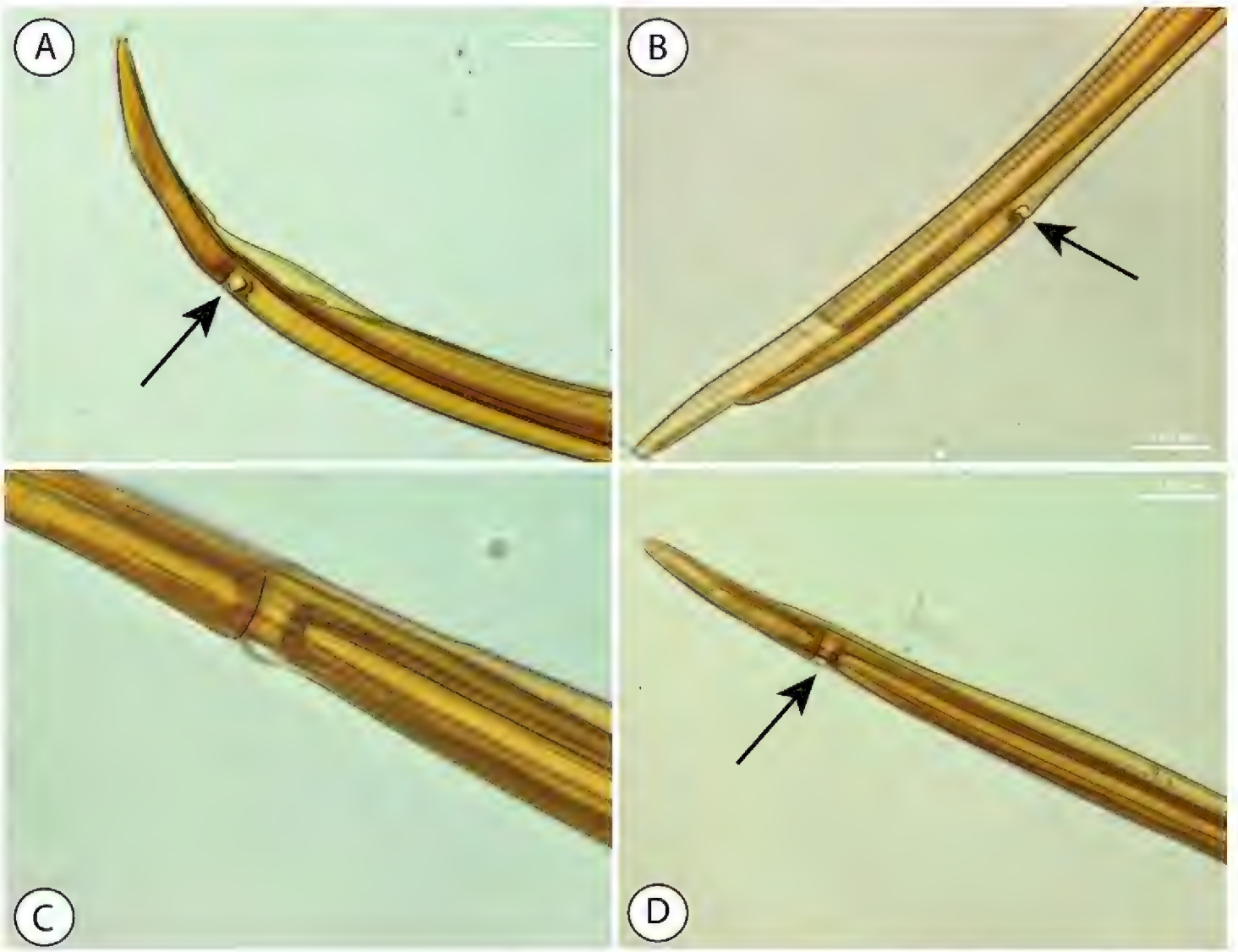

Figure 4. Comparison of the ovipositor clip between *G. lupini* (**A, C**) and *G. kimorum* (**B, D**). **A** *G. lupini* ovipositor tip, lateral view **B** *G. kimorum*, ovipositor tip, lateral view **C** *G. lupini* ventral of ovipositor showing ovipositor clip and membrane **D** *G. kimorum* ventral of ovipositor showing ovipositor clip and membrane. Black arrows indicate the location of the ovipositor clip.

mead [first label]; *Hexamerocera brasiliensis* male/female symbol Ashm (over) [front side, second label] ex *Drosophila punctata* fruitfly [back side, second label]; Paratype [third label, red]; *Eucoila* (*Hexamerocera*) *brasiliensis* Ihering [fourth label, in Weld's hand]; *Pseudeucoila brasiliensis* (R.v. Ihr.) [fifth label, Weld's hand); EUCOILIDAE *Eucoila brasiliensis* [white computer generated label]; USNMENT01119745. Deposited in USNM.

Other material examined. **Panama**: Monte Oscuro, June-July '95 [1895] Z-5203, USNMENT01119746 (male); USNMENT01119747 (female); Panama City, Z-3661 [no date]; 2 male specimens/ pin: USNMENT01119748–USNMENT01119749, USNMENT01119740–USNMENT01119742; Canal Zone, Balboa, VI.10.1936, J Zetek, collector, P.R. no. 1803; 4 females: USNMENT01119645–USNMENT01119648; 3 males: USNMENT01119649, USNMENT01119743, USNMENT01119744; Monte Oscuro, Panama City, Z-3666 [no date]; 1 female: USNMENT01119650; Monte Oscuro, Panama City, Z-3665 [no date]; 1 female: USNMENT01119651; Monte Oscuro, Panama City, Z-3665, ex *Anastrepha acidusa*, emerge 2–3 weeks after last fly out-25 days after pupation [no date]; 1 female:

USNMENT01119652; Ancon, Canal Zone, Z-2748, Ex *Anastrepha fratercula* or *Drosophila striata*, July 1927, I. Molino, collector; 2 females: USNMENT01119653 and USNMENT01119654; Taboga Island, Sept. 30, 1926, I. Molino, collector, Z-2727; 11 females: USNMENT01119656–USNMENT01119665, 1male: USNMENT01119666; Panama City, Z-3222, Ex *Anastrepha serpentina* in nispero, May 1930, J Zetek, collector; 2 males: USNMENT01119667, USNMENT01119668; Ancon, Canal Zone, Z-2715, Oct. 12, 1926, bred by Molina, ex fruit of *Spondias lutea*, parasite of diptera Z-2716; 1 female: USNMENT01119669. **Guadeloupe:** *Ganaspis* G. 302.1, Y. Carton; 3 females: USNMENT01119670–USNMENT01119672; 3 males USNMENT01119673–USNMENT01119675.

Cytochrome c oxidase subunit I (COI) Barcode region.

> Pseudoeucoila_brasiliensis_AP7BC36 (USNMENT01119647)

NNNNNNNNNNNNNNNNNNNNNAATTTGATCAGGAATAATTGGATCAAGTTTAAGAATAATTATTCGTCTAGAATTAGGCACCCCTTCACAATTAATTAATAATGATCAAATTTATAATACAATTGTTACCACTCATGCATTTGTAATAATTTTTTTTTATAGTAATACCAATTATAGTAGGAGGATTTGGAAATTACTTAATTCCCTTAATATTATCTGCCCCTGATATATCATTTCCTCGTCTTAATAATATAAGATTCTGATTATTAATTCCTTCTTTAATTTTAATAATTTCAAGTATATTTATTGATGAAGGATCTGGAACCGGATGAACCATTTATCCTCCTTTATCATTAAATAAATCACATCCAGGAATTTCAACTGATTTAGTAATTTTCTCCCTTCATCTTAGAGGAATTTCTTCAATTTTAGGATCAATTAATTTTATTGATGAAGGATCTGGAACCGGATGAACCATTTATCCTCCTTTATCATTAAATAAATCACATCCAGGAATTTCAACTGATTTAGTAATTTTCTCCCTTCATCTTAGAGGAATTTCTTCAATTTTAGGATCAATTAATTTTATTACAACTATTTTAAATATACGACCTAATTTTATAAGTATAGATAAAATTTCTTTATTTACTTGATCTATTTTTTCTTACTACCATTTTACTATTATTATCTTTACCAGTATTAGCAGGTGGAATCACTATATTTACTGTTTGATCGAAACATTAATACATCTTTTTATGATCCAATAGGAGGAGGTGACCCTATTCTATACCAACATTTATTC

>Ganaspis_brasiliensis_2966

TATATTATATTTTATTTTTTGGAATTTGATCAGGAATAATTGGATCAAGTTTAAGAATAATTATTCGACTAGAATTAGGCACCCCTTCACAATTAATTAATAATGATCAAATTTATAATACAATTGTTACCACTCATGCATTTGTAATAATTTTTTTTTATAGTAATACCAATTATAGTAGGAGGATTTGGAAATTACTTAATTCCTTTAATATTATCTGCCCCTGATATATCATTTCCTCGTCTTAATAATATAAGATTCTGATTATTAATCCCTTCTTTAATTTTAATAATTTCAAGTATATTTATTGATGAAGGATCTGGAACAGGATGAACAGTTTATCCTCCTTTATCATTAAATAAATCACATCCAGGAATTTCAACTGATTTAGTAATTTTCTCCCTTCATCTTAGAGGAATCTCTTCAATTCTAGGATCAATTAATTTTATTACAACTATTTTAAATATACGACCTAATTTTATAAGTATAGATAAAATTTCTTTATTTACTTGATCTATTTTTTCTTACTACCATTTTACTATTATTATCTTTACCAGTATTAGCAGGTGGAATCACTATATTACTGTTTGATCGAAACATTAATACATCTTTTTATGATCCAATAGGAGGAGGTGACCCTATTCTATACCAACATTTATTC

>Ganaspis_brasiliensis_2919
TATATTATATTTTATTTTTGGAATTTGATCAGGAATAATTGGATCAA-
GTTTAAGAATAATTATTCGACTAGAATTAGGCACCCCTTCACAAT-
TAATTAATAATGATCAAATTTATAATACAATTGTTACCACTCATGCATTT-
GTAATAATTTTTTTTATAGTAATACCAATTATAGTAGGAGGATTTG-
GAAATTACTTAATTCCTTTAATATTATCTGCCCCTGATATATCATTTC-
CTCGTCTTAATAATATAAGATTCTGATTATTAATCCCTTCTTTAATTT-
TAATAATTTCAAGTATATTTATTGATGAAGGATCTGGAACAGGATGAA-
CAGTTTATCCTCCTTTATCATTAAATAAATCACATCCAGGAATTTCAACT-
GATTTAGTAATTTTCTCCCTTCATCTTAGAGGAATCTCTTCAATTCTAG-
GATCAATTAATTTTATTACAACTATTTTAAATATACGACCTAATTTTATAA-
GTATAGATAAAATTTCTTTATTTACTTGATCTATTTTTCTTACTAC-
CATTTTACTATTATTATCTTTACCAGTATTAGCAGGTGGAATCACTATAT-
TACTGTTTGATCGAAACATTAATACATCTTTTTATGATCCAATAGGAG-
GAGGTGACCCTATTCTATACCAACATTTATTC

Biology. Kionobiont endoparasitoid of *Drosophila melanogaster*, *D. simulans*, and other *Drosophila* in decaying fruit. Original description and some label data suggesting *Anastrepha* (Tephritidae) as a host are most likely to represent erroneous associations (cf. Buffington and Forshage 2016).

***Ganaspis lupini* Buffington, sp. nov.**
https://zoobank.org/9CD88092-9D40-4C1D-BEBD-C15AAA722B39
Figs 1B, 3C, D, 4C, F

Diagnosis. Separated from *G. brasiliensis* by the completely smooth lateral aspect of the scutellum (Fig. 3C). Separated from *G. kimorum* by a well-developed ovipositor clip that is expanded across more than half the width of the ovipositor valve (Fig. 4C); in *G. kimorum*, the clip is smaller and does not extend past the midwidth of the ovipositor valve (Fig. 4E, F).

Description. As in description for *G. brasiliensis* species complex, but with the lateral aspect of the scutellum completely smooth; ovipositor clip large, extending beyond the halfway point across the fused ovipositor valve. Previous studies referencing 'Gb G3' or 'G3' refer to this species (Nomano et al. 2017; Giorgini et al. 2018; Abram et al. 2022).

Material examined. Holotype. **Japan:** Nagano, Yamanouchi, Shiga Kogen Hasuike Ski Resort 36.7189°N, 138.4935°E ex *D. suzukii*, *D. subpulchrella* on *Vaccinium* spp. 17 Aug 2017 Kenis, collector G3_Nagano, USNMENT01867461. Deposited in USNM. Paratypes. **Japan:** Nagano, Yamanouchi, Shiga Kogen Hasuike Ski Resort 36.7189°N, 138.4935°E ex *D. suzukii*, *D. subpulchrella* on *Vaccinium* spp. 17 Aug 2017 Kenis, collector G3_Nagano: USNMENT01867461, USNMENT01867462;

Tokyo Kimura Lab, field collected *G. xanthopoda* '*lutescens* type' Received USNM July 2015 From culture in lab; USNMENT00877742, USNMENT00877792, USNMENT00877779; Tokyo, Hachioji Naganuma Park 35.6368°N, 139.3647°E, INRA GO fruit on ground 16 Jun 2017 Girod, collector; USNMENT01734716, USNMENT01734717, USNMENT01734719, USNMENT01734696, USNMENT01025529, USNMENT01734695. **China:** Yunnan, Kunming Multiple sites in suburbs 25.0986°N, 102.8350°E ex *D. suzukii*, *D. pulchrella* on *Rubus foliosus*, *Fragraria moupinensis Sambucus adnate*; 16 Jul 2017; Daane, Hoelmer, Wang, collectors; ARS Colony, Newark voucher G3_Yunnan; USNMENT01867450–USNMENT01867453; Yunnan, Kunming, Chang Chong Shan, Wu Hua District, 25.132223°N 102.706662°E, 2207m, ex *D suzukii* on *Rubus foliosus*; collected 12.VII.2016, Giorgino and Guerreiri DSZ187; USNMENT01025535; Yunnan, Kunming, Dong Da Cun, Pan Long District, 25.098602°N 102.835000°E, 2239m, ex *D suzukii* on *Sambucus adnata*; collected 25.VII.2016, emerged 24.VIII.2016 Giorgino and Guerreiri DSZ130 (USNMENT01025534); Yunnan, Shiping, ex *D. suzukii/Myrica rubra*; 15 Jun 2017 Kenis, collector CABI colony voucher G3_Shiping; USNMENT01867471, USNMENT01867470. Paratypes deposited in USNM.

Etymology. This species is named in honor of the manga character "*Lupin the Third*" (MonkeyPunch 1967). The name reflects the 'G3' naming convention of this species, as well as Lupin the Third's personality as professional thief that sometimes tries to do good. We think *G. lupini* is certainly proficient in attacking SWD, but does not attack the most destructive stage of this pest fly.

Cytochrome c oxidase subunit I (COI) Barcode region.

>Ganaspis_lupini_GB86
TATATTATATTTTATTTTTGGAATTTGATCAGGAATAATTGGATCAA-
GTTTAAGAATAATTATTCGACTAGAATTAGGTACCCCTTCACAAT-
TAATTAATAATGATCAAATTTATAATACAATTGTAACCACTCATGCATTT-
GTAATAATTTTTTTTTATAGTAATACCAATTATAGTAGGAGGATTTG-
GAAATTATTTAATTCCCTTAATATTATCTACCCCTGATATATCATTTC-
CTCGTCTCAATAATATAAGATTCTGATTATTAATTCCTTCTTTAATTT-
TAATAATTTCAAGTATATTTATTGATGAAGGATCTGGAACCGGATGAA-
CAGTTTATCCTCCTTTATCATTAAATAAATCACACCCAGGAATTTCAACT-
GATTTAGTAATTTTCTCCCTTCATCTTAGAGGAATTTCTTCAATTCTAG-
GATCAATTAATTTTATTACAACTATTTTAAATATACGACCTAATTTTATAA-
GTATAGATAAAATTTCTTTATTTACTTGATCTATTTTTCTTACTAC-
CATTTTATTATTATTATCTTTACCAGTATTAGCAGGTGGAATTACTATAT-
TACTATTTGACCGAAACATTAATACATCTTTTTATGACCCAATAGGAG-
GAGGTGACCCTATTCTATACCAACATTTATTC

>Ganaspis_lupini_BBP860
TATATTATATTTTATTTTTGGAATTTGATCAGGAATAATTGGATCAA-
GTTTAAGAATAATTATTCGACTAGAATTAGGTACCCCTTCACAAT-
TAATTAATAATGATCAAATTTATAATACAATTGTAACCACTCATGCATTT-

GTAATAATTTTTTTTATAGTAATACCAATTATAGTAGGAGGATTTG-
GAAATTATTTAATTCCCTTAATATTATCTACCCCTGATATATCATTTC-
CTCGTCTCAATAATATAAGATTCTGATTATTAATTCCTTCTTTAATTT-
TAATAATTTCAAGTATATTTATTGATGAAGGATCTGGAACCGGATGAA-
CAGTTTATCCTCCTTTATCATTAAATAAATCACACCCAGGAATTTCAACT-
GATTTAGTAATTTTCTCCCTTCATCTTAGAGGAATTTCTTCAATTCTAG-
GATCAATTAATTTTATTACAACTATTTTAAATATACGACCTAATTTTATAA-
GTATAGATAAAATTTCTTTATTTACTTGATCTATTTTTCTTACTAC-
CATTTTATTATTATTATCTTTACCAGTATTAGCAGGTGGAATTACTATAT-
TACTATTTGACCGAAACATTAATACATCTTTTTATGACCCAATAGGAG-
GAGGTGACCCTATTCTATACCAACATTTATTC

Biology. Koinobiont endoparasitoid of *Drosophila lutescens*, *D. rufa*, and *D. biauraria* (Mitsui and Kimura 2010). Nomano et al. (2017) indicate this species does not oviposit into *D. suzukii*, but Seehausen et al. (2020) recorded successful parasitism of *D. suzukii* by *'Ganaspis* cf. *brasiliensis'* G3, and we consider this a trustworthy host record.

***Ganaspis kimorum* Buffington, sp. nov.**

https://zoobank.org/330D215F-8FEA-4D7B-8D80-C409DC2C4199

Figs 1C, 2, 3E, F, 4B, D, E

Material examined. Holotype. **Japan:** Tokyo Kimura Lab, field collected *G. xanthopoda 'suzukii* type' Collected June 2010 Received USNM July 2015; female, USNMENT00877810. Deposited in USNM. Paratypes: **Japan:** Tokyo Kimura Lab, field collected *G. xanthopoda 'suzukii* type' Collected June 2010 Received USNM July 2015; USNMENT00877811, USNMENT00877772, USNMENT00877823; Kanto Province, Tokyo district, Hachioji, Naganuma Park 35°38'12"N, 139°21'54"E Ex larva of *Drosophila suzukii* Coll. 3.VI.2015, Leg. N. Ris & P. Girod; USNMENT 01025537–USNMENT01025541; Tokyo, Hachioji Naganuma Park 35.6368°N,139.3647°E, ex *D. suzukii* on *Prunus serrulata* 16 Jun 2017; Girod, collector CABI colony voucher G1_Tokyo; USNMENT01867459, USNMENT01867458, USNMENT01025536. **China:** Yunnan Province, Kunming district, Kunming, Yunnan Agricultural University, 25°07'41"N, 102°44'50"E, Ex larva of *Drosophila suzukii* Coll. 3.VI.2015, Leg. M. Kenis; USNMENT01025542–USNMENT01025546; Yunnan Province, Honghe district, Shiping 23°41'15"N, 102°32'53"E Ex larva of *Drosophila suzukii* Coll. 6.VI.2015, Leg. M. Kenis; USNMENT01025547–USNMENT01025551; Yunnan Province, Kunming district, Kunming, Yunnan Agricultural University 25°07'41"N, 102°44'50"E Ex larva of *Drosophila suzukii* Coll. 3.VI.2015, Leg. M. Kenis; USNMENT01025552, USNMENT01025553;USNMENT01734709;Yunnan,KunmingXiningTemple25.1072°N, 102.7167°E, ex *D. suzukii/ D. pulchrella*; on *Prunus* sp.; 17 May 2017 Kenis, collector CABI colony voucher G1_Yunnan; USNMENT01867468, USNMENT01867467, USNMENT01867454–USNMENT01867457, USNMENT01025528. Yunnan Prov-

ince, Honghe district, Shiping 23°41'15"N, 102°32'53"E Ex larva of *Drosophila suzukii* Coll. 6.VI.2015, Leg. M. Kenis; USNMENT01734706, USNMENT01734705, USNMENT01025530, USNMENT01734714. Yunnan, Kunming, Dong Da Cun, Pan Long District, 25.098602°N 102.835000°E, 2239m, ex *D. suzukii* on *Sambucus adnata*; collected 25.VII.2016, emerged 24.VIII.2016 Giorgino and Guerreiri DSZ118, DSZ137, DSZ188; USNMENT01025531–USNMENT01025533; Yunnan, Dali, ex *D. suzukii*/ *Sambucus williamsii*; 16 Jun 2017 Kenis, collector CABI colony voucher G1_Dali; USNMENT01867465, USNMENT01867466. Paratypes deposited in USNM.

Diagnosis. Separated from *G. brasiliensis* by the completely smooth lateral aspect of the scutellum (Fig. 3E). Separated from *G. lupini* by the less-developed ovipositor clip that does not extend past the midwidth of the ovipositor valve (Fig. 4B, E). In *G. lupini* the ovipositor clip expands across more than half the width of the ovipositor valve (Fig. 4C).

Description. As in description for *G. brasiliensis* species complex, but with the lateral aspect of scutellum completely smooth; ovipositor clip reduced, not extending beyond the halfway point across the fused ovipositor valve. Previous studies referencing 'Gb G1' or 'G1' refer to this species (Nomano et al. 2017; Giorgini et al. 2018; Abram et al. 2022).

Etymology. Named in honor of Prof. Kimura (Hokkaido University, retired) and Dr Kim Hoelmer (USDA-ARS, retired). The name is a combination of Kimura and Kim Hoelmer.

Cytochrome c oxidase subunit I (COI) Barcode region.

>Ganaspis_kimorum_BBP857
NATATTATATTTTATTTTTGGTATTTGATCAGGAATAATTGGATCAA-
GTTTAAGAATAATTATTCGATTAGAATTAGGAACCCCTTCACAAT-
TAATTAATAATGATCAAATTTATAATACAATTGTTACTACTCATGCATTT-
GTAATAATTTTTTTTTATAGTTATACCAATTATAGTTGGAGGATTTG-
GAAATTACTTAATTCCTTTAATATTATCTGCTCCTGATATATCATTCC-
CTCGTCTTAATAATATAAGATTTTGATTATTAATCCCTTCTTTAATTT-
TAATAATTTCAAGTATATTTATTGATGAAGGGTCTGGAACTGGATGAACA-
GTTTATCCTCCTTTATCACTAAATAAGTCCCACCCAGGAATCTCAACT-
GACTTAGTAATTTTTTCTCTTCATCTTAGAGGAATTTCTTCAATTTTAG-
GATCAATTAATTTTATTACAACTATTCTAAATATACGACCAAATTTAATAA-
GTATAGATAAAATTTCTTTATTTACTTGATCCATTTTTTCTTACCAC-
TATTTTATTATTATTATCTTTACCAGTATTAGCAGGTGGAATCACTATAT-
TACTTTTTGACCGAAATATTAATACATCTTTTTATGACCCAATAGGAG-
GAGGAGACCCAATTCTATACCAACACTTATTT

>Ganaspis_kimorum_233137974_E02 (partial sequence, 592 bp)
ATTAGAATTAGGAACCCCTTCACAATTAATTAATAATGATCAAATT-
TATAATACAATTGTTACTACTCATGCATTTGTAATAATTTTTTTTTATAGT-
TATACCAATTATAGTTGGAGGATTTGGAAATTACTTAATTCCTTTAATAT-
TATCTGCTCCTGATATATCATTCCCTCGTCTTAATAATATAAGATTTTGAT-
TATTAATCCCTTCTTTAATTTTAATAATTTCAAGTATATTTATTGATGAA-
GGGTCTGGAACTGGATGAACAGTTTATCCTCCTTTATCACTAAATAA-

GTCCCACCCAGGAATCTCAACTGACTTAGTAATTTTTTCTCTTCATCT-
TAGAGGAATTTCTTCAATTTTAGGATCAATTAATTTTATTACAAC-
TATTCTAAATATACGACCAAATTTAATAAGTATAGATAAAATTTCTT-
TATTTACTTGATCCATTTTTCTTACCACTATTTTATTATTATTATCTT-
TACCAGTATTAGCAGGTGGAATCACTATATTACTTTTTGACCGAAATAT-
TAATACATCTTTTTATGACCCAATAGGAGGAGGAGACCCAATTCTATAC-
CAACACTTATTT

>Ganaspis_kimorum_233137957_F06
NATATTATATTTTATTTTTGGTATTTGATCAGGAATAATTGGATCAA-
GTTTAAGAATAATTATTCGATTAGAATTAGGAACCCCTTCACAAT-
TAATTAATAATGATCAAATTTATAATACAATTGTTACTACTCATGCATTT-
GTAATAATTTTTTTTATAGTTATACCAATTATAGTTGGAGGATTTG-
GACATTACTTAATTCCTTTAATATTATCTGCTCCTGATATATCATTCC-
CTCGTCTTAATAATATAAGATTTTGATTATTAATCCCTTCTTTAATTT-
TAACAATTTCAAGTATATTTATTGATGAAGGATCTGGAACCGGATGAACA-
GTTTATCCTCCTTTATCACTAAATAAGTCCCACCCAGGAATCTCAACT-
GACTTAGTAATTTTTTCTCTTCATCTTAGAGGAATTTCTTCAATTTTAG-
GATCAATTAATTTTATTACAACTATTCTAAATATACGACCAAATTTAATAA-
GTATAGATAAAATTTCTTTATTTACTTGATCCATTTTTCTTACCAC-
TATTTTATTATTATTATCTTTACCAGTATTAGCAGGTGGAATCACTATAT-
TACTTTTTGACCGAAATATTAATACATCTTTTTATGACCCAATAGGAG-
GAGGAGACCCAATTCTATACCAACACTTATTT

Biology. Koinobiont endoparasitoid of *Drosophila suzukii* (Nomano et al. 2017; Girod et al. 2018b; Wang et al. 2018; Seehausen et al. 2020; Daane et al. 2021). Seehausen et al. (2020) found '*Ganaspis* cf. *brasiliensis*' G1 could successfully parasitize *D. melanogaster* in lab culture.

Discussion

The logic behind this comprehensive phylogenetic species delimitation study is based on observations that COI can sometimes be error-prone in species discrimination in Eucoilinae, as well as other insect groups (Brower 2006; Lohse 2009; Goldstein and LaSalle 2011; Collins and Cruickshank 2012), sometimes mediated by the presence of *Wolbachia* (Jiggins 2003; Klopfstein et al. 2016; Cariou et al. 2017). When we compared our trees with the basic topology of Nomano et al. (2017), which relied on COI and ITS2 for discriminating the 'G-species', we find some disagreement with respect to phylogeny. The former G3 (now *G. lupini*) is recovered as the sister-group to *G. brasiliensis*, and G1 (now *G. kimorum*) is recovered as sister-group to the clade containing *G. brasiliensis*+*G. lupini*. As our dataset is more comprehensive than that of Nomano et al. (2017), both in terms of taxon sampling and number of loci, we suggest the tree pre-

sented here is a more accurate interpretation of the evolution of this group. While the use of UCE markers coupled with nex-gen sequencing technology has made generating larger amounts of data much easier and more affordable, there is still a place for mitochondrial 'barcode' data with respect to determining these cryptic species. We *strongly* encourage newly generated barcode data to be only compared to barcode data here in this paper, as well as barcode data in the *Drosophila* parasitoid database DROP (Lue et al. 2021) where sequences are backed by authoritatively identified voucher specimens.

The dataset here has yielded more nuanced results concerning in-group relationships than previous studies of these taxa. For instance, *Ganaspis lupini* has three distinct subclades within the species; we have decided to retain these three clades as members of the same species. Within *Ganaspis brasiliensis*, even more subclades can be discerned, some of which may eventually be split out into additional species. The ratio of the intra vs inter pairwise tree distances (Table 1 and Suppl. material 1: table S5) suggests that members of both *G. brasiliensis* and *G. lupini* seem to be more diverse compared to members within of *G. kimorum*. However, unlike the situation between *G. brasiliensis*, *G. lupini* and *G. kimorum*, where morphological differences were noted, though difficult to observe, there are no such morphological differences among the clades of *G. brasiliensis*. Hence, for the present time, we are considering all these subclades to be members of *G. brasiliensis*. It would have been very interesting to consider UCE data from types of *G. brasiliensis*, but unfortunately, attempts at amplifying extracts from the type series yield low-quality UCE data.

Biogeographically, *G. brasiliensis* appears to be a pan-tropical species, and seemingly no specimens of this species have been collected outside the subtropics (with Hawai'i being the most 'temperate' locality), while *Ganaspis lupini* and *G. kimorum* appear to be temperate species.

This appears to be the first study to utilize the ovipositor clip for species-level discrimination. Prior to this study, the clip was formally described (van Lenteren et al. 1998), followed by Buffington (2007) where the presence/absence of the clip across Figitidae was examined. Buffington (2007) hypothesized that the absence of the clip in Aspicerinae and Anacharitinae was linked to a 'quick-strike' oviposition strategy, as the hosts they attacked (Syrphidae and Hemerobiidae, respectively) are themselves aggressive hosts to be attacking. Further, the Charipinae are hyperparasitoids of aphidophagous braconids and chalcidoids, where there is no need for host restraint. Finally, the leaf-miner specialists, among the eucoiline Zaeucoilini and Diglyphosematini, also lack the clip as their host is a 'captive audience' that cannot readily escape parasitization. Together, these data suggest the ovipositor clip, in the appropriate circumstance, is an asset; in other circumstances, a liability.

The pattern observed in the *Ganaspis brasiliensis* species complex can be interpreted along the same lines. In the case of both *G. brasiliensis* and *G. lupini*, the ovipositor clip has retained its typical size, spanning the width and depth of the fused valve of the ovipositor (Figs 4, 5). By contrast, *G. kimorum* has a much-reduced ovipositor clip, so much reduced that the last author had to mount some 40 ovipositors before the nature of the reduced clip could actually be observed (in some cases, there appeared to be no

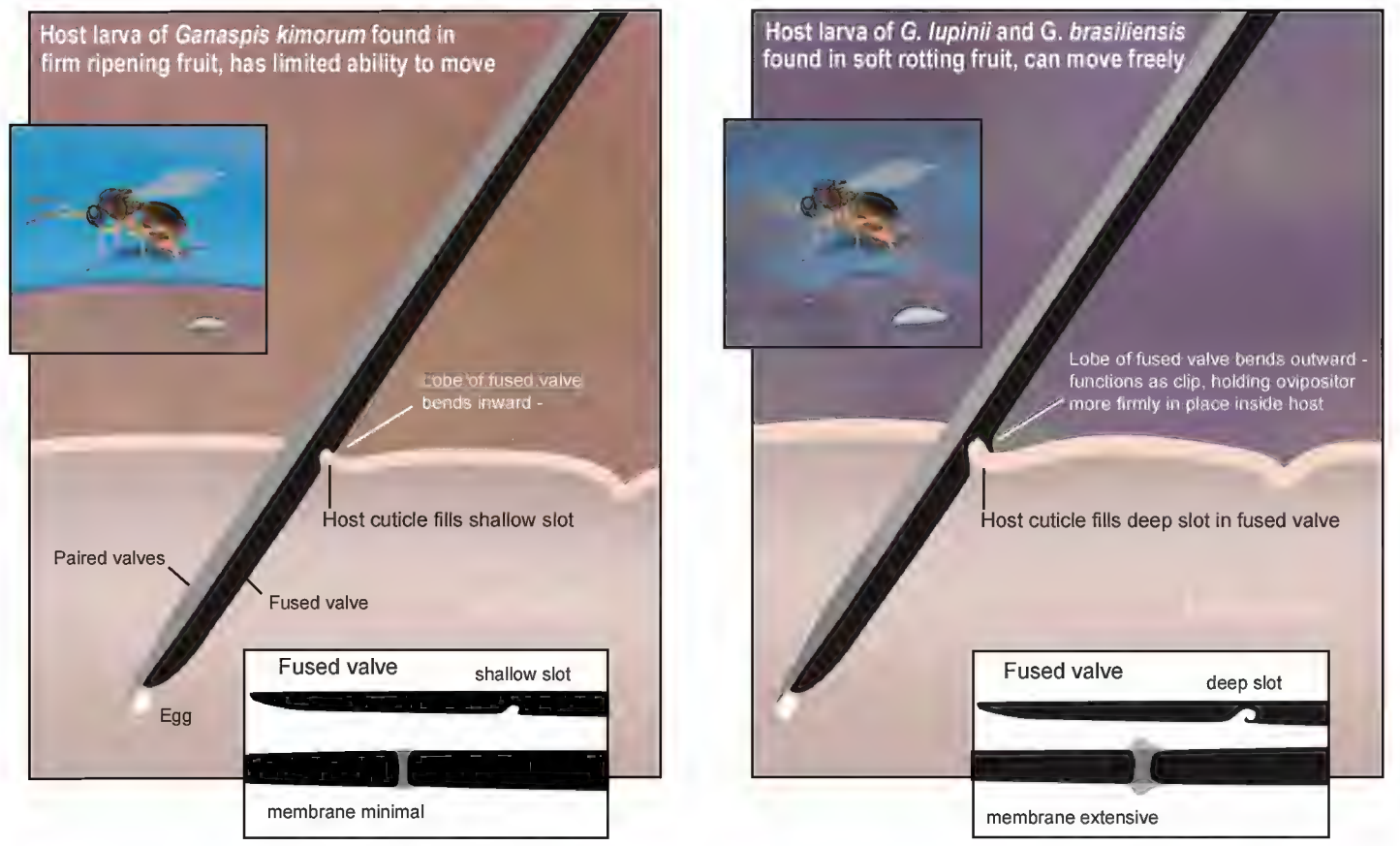

Figure 5. Functional morphology of the ovipositor clip.

ovipositor clip present) (Fig. 4). Both *G. brasiliensis* and *G. lupini* are attacking hosts within an already decomposing substrate, allowing the would-be host ample room for escape. Further, the skin of the fruit, if still intact, would be very soft, and the clip itself would not be engaged by it. In the case of *G. kimorum*, which attacks its host in ripe fruit, the host larvae would have much less space for escape. Further, as the skin of the fruit is still intact, this more rigid barrier may in fact cause complications for the insertion of the ovipositor, as the clip itself may in fact snag on the fruit skin during insertion. The reduction of the clip into a much more streamlined silhouette, we hypothesize, helps the ovipositor insert into the fruit more effectively and not engage the fruit skin. And, as the host larvae has a reduced chance of escape inside of fresh fruit, this shallower ovipositor clip remains effective at securing the host (Fig. 5).

What is the future of species delimitation using UCE data? We have demonstrated here that these data are quite effective at discriminating among morphologically virtually identical but biologically distinct species. We may very well be observing the immediate after-effects of speciation, where morphological characters have not yet manifested themselves to be observed, but clearly, biological and genetic characters distinguishing these species are present. And if this is the case, the much larger amount of sequence data per specimen that UCE methodology provides is rather critical. As the cost of this technique continues to decline, we predict this technique will certainly be considered more closely in the future.

Perhaps a more difficult question to consider is: what is the future of *Ganaspis* taxonomy? *Ganaspis* currently has only 49 nominal species, of which 17 actually belong in other genera and are awaiting new combinations, while 8 are *nomina inquirenda*, the types of which have never been studied by modern researchers, leaving 24 described

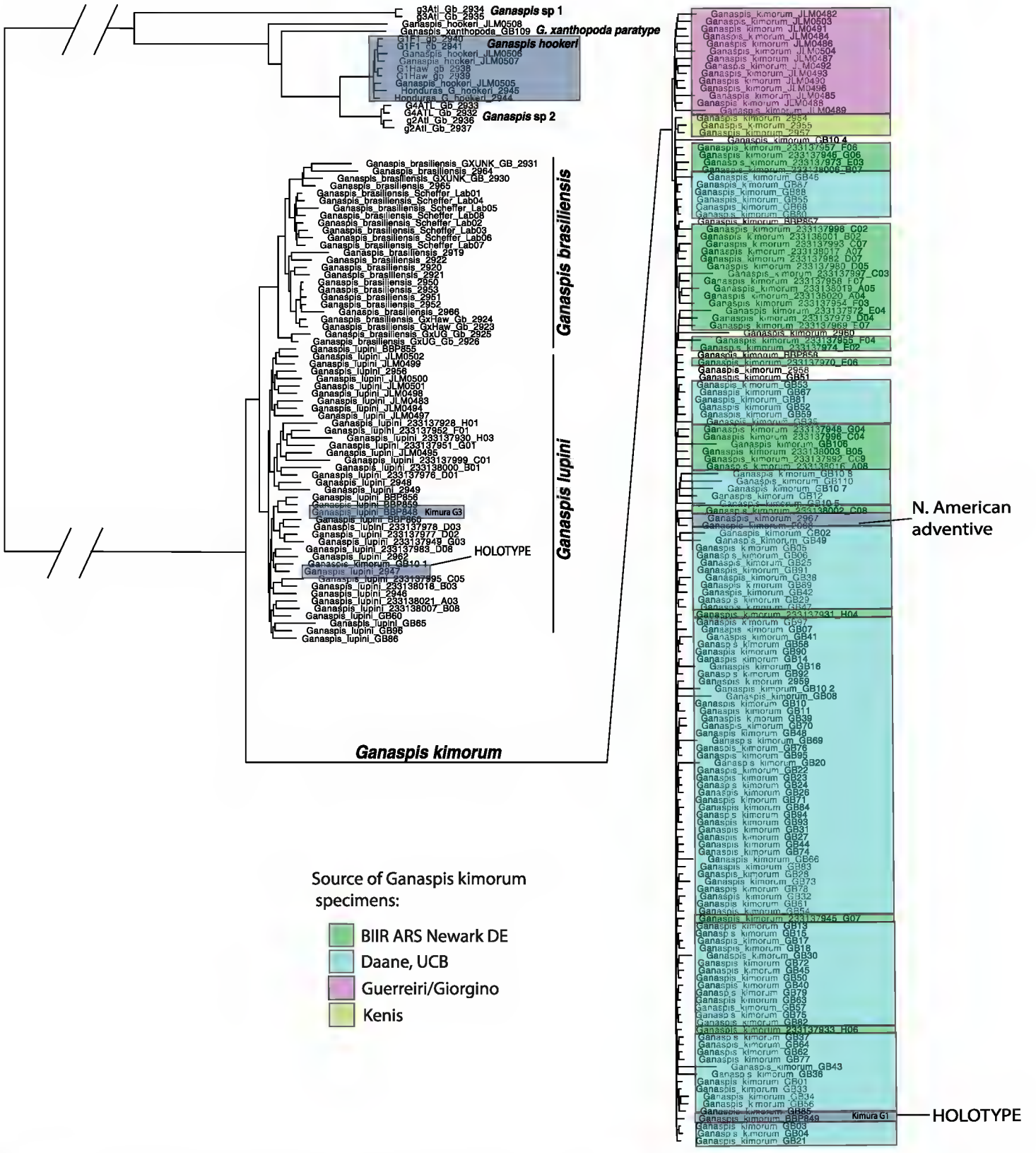

Figure 6. Phylogeny of the *Ganaspis brasiliensis* species complex based on the SYMTEST analysis. Specific populations, mentioned in previous studies, are highlighted by arrows, as well as where the holotypes of the two new species are located. The adventive population in British Columbia is also noted.

Ganaspis species. But then there are an additional 46 *Ganaspis* species that are currently classified in other genera and await new combinations in *Ganaspis* (unpublished data). On top of this there are numerous undescribed species, including a remarkable number of 'BINs' in BOLD (Sosa-Calvo and Buffington, pers. obsv.) But these considerations are all based on current circumscription where it seems very likely that *Ganaspis* is at least a paraphyletic assemblage of all the "typical Ganaspini" without certain striking apomorphies which define related genera such as *Areaspis* Lin, 1988, *Didyctium* Riley, 1879, *Discaspis* Lin, 1988, *Endecameris* Yoshimoto, 1963, *Gastraspis* Lin, 1988 and

Hexacola Föster, 1869 (cf. the keys in van Noort et al. 2014; Buffington and Forshage 2015). But there is also a possibility that this represents a morphology that several lineages have been converging into based on similar life histories (the similarity between different *Ganaspis* and *Leptopilina* species attacking similar drosophilid hosts is rather striking, considering that *Leptopilina* belongs to an entirely different group within Eucoilinae (the tribe Eucoilini)). Indeed, in all published phylogenetic analyses where it has been tested, *Ganaspis* has come out non-monophyletic (Fontal-Cazalla et al. 2002; Buffington et al. 2007; Blaimer et al. 2020). Whether the genus is indeed a paraphyletic grouping of the more plesiomorphic crown-group Ganaspini, or rather a polyphyletic assemblage of wasps having converged on a similar morphology, is very difficult to say, and is perhaps not even a very meaningful question to ask before a more rigid circumscription of the genus has been attained. A global review of the genus is desperately needed to give it a meaningful circumscription and to identify monophyletic species groups which can be properly revised. Perhaps the new UCE methodology can assist, especially since UCE can be generated effectively from older museum specimens.

In conclusion, working out the limits of these three species of *Ganaspis*, like in other cases of cryptic species complexes, has required a great deal of behavioral study, genetic study, and morphological study, and benefitted from the reciprocal illumination they have offered. This has also involved researchers from around the world, conducting very careful work documenting these species, as well as the centralization of voucher specimens such that various lines of evidence can be directly, and quickly, compared. Thus, this work represents a celebration of international collaboration between research groups in different countries with different specializations for an integrated solution to independently noted problems.

Acknowledgements

Collectively we would like to thank the following people and groups for providing the specimens, and data, needed to complete this project: members of the ARS-BIIR group in Newark, DE; the Daane Lab, UC Berkeley; Abram Lab, Agassiz Research and Development Centre, Agassiz, British Columbia, Canada; M. Giorgino and E. Guerrieri, Institute for Sustainable Plant Protection, National Research Council of Italy, via Università 133, 80055 Portici, Italy; and the Kimura Lab, Hokkaido University, Sapporo, Japan. Jim Woolley (retired, Texas A&M), Fredrik Ronquist (Naturhistoriska riksmuseet, Stockholm, Sweden) and combined SI-USDA Hymenoptera Unit at NMNH helped flesh out ideas and concepts presented here. JSC was financially supported by the National Science Foundation grants DEB 1754242 and DEB 1927161, and would like to thank Sean Brady and Ted Schultz (Department of Entomology, NMNH). The editor, Miles Zhang, and the two reviewers, Mar Ferrer-Suay and Simon van Noort, helped improve this manuscript. Mention of trade names or commercial products in this publication is solely for the purpose of providing specific information and does not imply recommendation or endorsement by the USDA. USDA is an equal opportunity provider and employer.

References

Abram PK, McPherson AE, Kula R, Hueppelsheuser T, Thiessen J, Perlman SJ, Curtis CI, Fraser JL, Tam J, Carrillo J, Gates M, Scheffer S, Lewis M, Buffington M (2020) New records of *Leptopilina*, *Ganaspis*, and *Asobara* species associated with *Drosophila suzukii* in North America, including detections of *L. japonica* and *G. brasiliensis*. Journal of Hymenoptera Research 78: 1–17. https://doi.org/10.3897/jhr.78.55026

Abram PK, Wang X, Hueppelsheuser T, Franklin MT, Daane KM Lee JC, Lue CH, Girod P, Carrillo J, Wong WHL, Kula RR, Gates MW, Hogg B, Moffat CE, Hoelmer KA, Sial AA, Buffington ML (2022) A Coordinated Sampling and Identification Methodology for Larval Parasitoids of Spotted-Wing *Drosophila*. Journal of Economic Entomology 115: 922–942. https://doi.org/10.1093/jee/toab237

Alex Smith M, Fernández-Triana JL, Eveleigh E, Gómez J, Guclu C, Hallwachs W, Hebert PD, Hrcek J, Huber JT, Janzen D, Mason PG, Miller S, Quicke DL, Rodriguez JJ, Rougerie R, Shaw MR, Várkonyi G, Ward DF, Whitfield JB, Zaldívar-Riverón A (2013) DNA barcoding and the taxonomy of Microgastrinae wasps (Hymenoptera, Braconidae): impacts after 8 years and nearly 20 000 sequences. Molecular Ecology Resources 13: 168–176. https://doi.org/10.1111/1755-0998.12038

Bankevich A, Nurk S, Antipov D, Gurevich AA, Dvorkin M, Kulikov AS, Lesin V, Nikolenko S, Pham S, Prjibelski A, Pyshkin A, Sirotkin A, Vyahhi N, Tesler G, Alekseyev M, Pevzner P (2012) SPAdes: A new genome assembly algorithm and its applications to single-cell sequencing. Journal of Computational Biology 19(5): 455–477. https://doi.org/10.1089/cmb.2012.0021

Barrera CA, Sosa-Calvo J, Schultz TR, Rabeling C, Bacci Jr M (2022) Phylogenomic reconstruction reveals new insights into the evolution and biogeography of *Atta* leaf-cutting ants (Hymenoptera: Formicidae). Systematic Entomology 47: 13–35. https://doi.org/10.1111/syen.12513

Blaimer BB, Santos BF, Cruaud A, Gates MW, Kula RR, Mikó I, Rasplus JY, Smith D, Talamas E, Brady S, Buffington M (2023) Key innovations and the diversification of Hymenoptera. Nature Communications 14: 1212. https://doi.org/10.1038/s41467-023-36868-4

Blaimer BB, Gotzek D, Brady S, Buffington ML (2020) Comprehensive phylogenomic analyses re-write the evolution of parasitism within cynipoid wasps. BMC Evolutionary Biology 20: 1–22. https://doi.org/10.1186/s12862-020-01716-2

Borowiec ML (2019) Spruceup: fast and flexible identification, visualization, and removal of outliers from large multiple sequence alignments. Journal of Open Source Software 4: 1635. https://doi.org/10.21105/joss.01635

Branstetter MG, Danforth BN, Pitts JP, Faircloth BC, Ward PS, Buffington ML, Gates MW, Kula RR, Brady SG (2017) Phylogenomic Insights into the Evolution of Stinging Wasps and the Origins of Ants and Bees. Current Biology 27: 1019–1025. https://doi.org/10.1016/j.cub.2017.03.027

Branstetter MG, Muller A, Griswold TL, Orr MC, Zhu CD (2021) Ultraconserved element phylogenomics and biogeography of the agriculturally important mason bee subgenus *Osmia* (*Osmia*). Systematic Entomology 46: 453–472. https://doi.org/10.1111/syen.12470

Branstetter MG, Longino JT (2022) UCE phylogenomics of new world *Cryptopone* (Hymenoptera: Formicidae) elucidates genus boundaries, species boundaries, and the vicariant

history of a temperate–tropical disjunction. Insect Systematics and Diversity 6: 1–23. https://doi.org/10.1093/isd/ixab031

Brower AVZ (2006) Problems with DNA barcodes for species delimitation: 'ten species' of *Astraptes fulgerator* reassessed (Lepidoptera: Hesperiidae). Systematics and Biodiversity 4: 127–132. https://doi.org/10.1017/S147720000500191X

Buffington M (2007) The occurrence and phylogenetic implications of the ovipositor clip within the Figitidae (Insecta: Hymenoptera: Cynipoidea). Journal of Natural History 41 2267–2282. https://doi.org/10.1080/00222930701579732

Buffington ML Forshage M (2016) Redescription of *Ganaspis brasiliensis* (Ihering, 1905), new combination (Hymenoptera: Figitidae), a natural enemy of the invasive *Drosophila suzukii* (Matsumura, 1931) (Diptera: Drosophilidae). Proceedings of the Entomological Society of Washington 118: 1–13. https://doi.org/10.4289/0013-8797.118.1.1

Buffington ML, Nylander JAA, Heraty JM (2007) The phylogeny and evolution of Figitidae (Hymenoptera: Cynipoidea). Cladistics 23: 403–431. https://doi.org/10.1111/j.1096-0031.2007.00153.x

Bushnell Brian (2014) BBMap: A fast, accurate, splice-aware aligner, United States. https://www.osti.gov/services/purl/1241166

Cariou M, Duret L, Charlat S (2017) The global impact of *Wolbachia* on mitochondrial diversity and evolution. Journal of Evolutionary Biology 30: 2204–2210. https://doi.org/10.1111/jeb.13186

Castresana J (2000) Selection of conserved blocks from multiple alignments for their use in phylogenetic analysis. Molecular Biology and Evolution 17: 540–552. https://doi.org/10.1093/oxfordjournals.molbev.a026334

Chernomor O, von Haeseler A, Minh BQ (2016) Terrace aware data structure for phylogenomic inference from supermatrices. Systematic Biology 65: 997–1008. https://doi.org/10.1093/sysbio/syw037

Collins RA, Cruickshank RH (2012) The seven deadly sins of DNA barcoding. Molecular Ecology Resources 13: 969–975. https://doi.org/10.1111/1755-0998.12046

Faircloth BC, Branstetter MG, White ND, Brady SG (2015) Target enrichment of ultraconserved elements from arthropods provides a genomic perspective on relationships among Hymenoptera. Molecular Ecology Resources 15: 489–501. https://doi.org/10.1111/1755-0998.12328

Faircloth BC, Glenn TC (2012) Not All Sequence Tags Are Created Equal: Designing and Validating Sequence Identification Tags Robust to Indels. PLoS ONE 7(8): e42543. https://doi.org/10.1371/journal.pone.0042543

Fontal-Cazalla FM, Buffington M, Nordlander G, Liljeblad J, Ros-Farre´ P, Nieves-Aldrey JL, Pujade-Villar J, Ronquist F (2002) Phylogeny of the Eucoilinae (Hymenoptera: Cynipoidea: Figitidae). Cladistics 18:154–199. https://doi.org/10.1111/j.1096-0031.2002.tb00147.x

Giorgini M, Wang XG, Wang Y, Chen FS, Hougardy E, Zhang HM, Chen ZQ, Chen HY, Liu CX, Cascone P, Formisan G, Carvalho GA, Biondi A, Buffington ML, Daane KM, Hoelmer KA, Guerrieri E (2019) Exploration for native parasitoids of *Drosophila suzukii* in China reveals a diversity of parasitoid species and narrow host range of the dominant parasitoid. Journal of Pest Science 92: 509–522. https://doi.org/10.1007/s10340-018-01068-3

Glenn TC, Pierson TW, Bayona-Vasquez NJ, Kieran TJ, Hoffberg SL, Thomas JC, Lefever DE, Finger JW, Gao B, Bian X, Louha S, Kolli RT, Bentley KE, Rushmore J, Wong K, Shaw TI, Ro-

throck Jr MJ, McKee AM, Guo TL, Mauricio R, Molina M, Cummings BS, Lash LH, Lu K, Gilbert GS, Hubbell SP, Faircloth BC (2019) Adapterama II: universal amplicon sequencing on Illumina platforms (TaggiMatrix). PeerJ. 7: e7786. https://doi.org/10.7717/peerj.7786

Goldstein P, DeSalle R (2011) Integrating DNA barcode data and taxonomic practice: determination, discovery, and description. BioEssays: news and reviews in molecular, cellular and developmental biology 33: 135–147. https://doi.org/10.1002/bies.201000036

Guindon S, Dufayard J-F, Lefort V, Anisimova M, Hordijk W, Gascuel O (2010) New algorithms and methods to estimate Maximum-Likelihood phylogenies: Assessing the performance of PhyML 3.0. Systematic Biology 59: 307–321. https://doi.org/10.1093/sysbio/syq010

Hanisch PE, Sosa-Calvo J, Schultz TR (2022) The last piece of the puzzle: Phylogenetic position and natural history of the monotypic fungus-farming ant genus *Paramycetophylax* (Formicidae: Attini). Insect Systematics and Diversity 6: 1–17. https://doi.org/10.1093/isd/ixab029

Hansson C, Hambäck P (2013) Three cryptic species in *Asecodes* (Förster) (Hymenoptera, Eulophidae) parasitizing larvae of *Galerucella* spp. (Coleoptera, Chrysomelidae), including a new species. Journal of Hymenoptera Research 30: 51–64. https://doi.org/10.3897/jhr.30.4279

Heraty JM, Woolley JB, Hopper K, Hawks D, Kim JW, Buffington ML (2007) Molecular phylogenetics and reproductive incompatibility in a complex of cryptic species of aphid parasitoids. Molecular Phylogenetics and Evolution 45: 480–493. https://doi.org/10.1016/j.ympev.2007.06.021

Hoang DT, Chernomor O, von Haeseler A, Minh BQ, Vinh LS (2018) UFBoot2: Improving the Ultrafast Bootstrap Approximation. Molecular Biology And Evolution 35: 518–522. https://doi.org/10.1093/molbev/msx281

Hopper KR, Wang X, Kenis M, Seehausen ML, Abram PK, Daane KM, Buffington ML, Hoelmer KA, Kingham BF, Shevchenko O, Bernberg E (2024) Genome divergence and reproductive incompatibility among populations of *Ganaspis* near *brasiliensis*. G3: Genes, Genomes, Genetics: jkae090. https://doi.org/10.1093/g3journal/jkae090

Jiggins F (2003) Male-killing *Wolbachia* and mitochondrial DNA: Selective sweeps, hybrid introgression and parasite population dynamics. Genetics 164: 5–12. https://doi.org/10.1093/genetics/164.1.5

Kalyaanamoorthy S, Minh BQ, Wong TK, von Haeseler A, Jermiin LS (2017) ModelFinder: fast model selection for accurate phylogenetic estimates. Nature Methods 14: 587–589. https://doi.org/10.1038/nmeth.4285

Katoh K, Standley DM (2013) MAFFT multiple sequence alignment software version 7: Improvements in performance and usability. Molecular Biology And Evolution 30: 772–780. https://doi.org/10.1093/molbev/mst010

Katoh K, Kuma K-I, Toh H, Miyata T (2005) MAFFT version 5: Improvement in accuracy of multiple sequence alignment. Nucleic Acids Research 33: 511–518. https://doi.org/10.1093/nar/gki198

Katoh K, Standley DM (2014) MAFFT: iterative refinement and additional methods. Multiple Sequence Alignment Methods: 131–146. https://doi.org/10.1007/978-1-62703-646-7_8

Klopfstein S, Kropf C, Baur H (2016) *Wolbachia* endosymbionts distort DNA barcoding in the parasitoid wasp genus *Diplazon* (Hymenoptera: Ichneumonidae). Zoological Journal of the Linnean Society 177: 541–557. https://doi.org/10.1111/zoj.12380

Krueger F (2015) Trim Galore!: A wrapper around Cutadapt and FastQC to consistently apply adapter and quality trimming to FastQ files, with extra functionality for RRBS data. Babraham Institute. https://www.bioinformatics.babraham.ac.uk/projects/trim_galore/

Lue CH, Buffington ML, Scheffer S, Lewis M, Elliott TA, Lindsey AR, Driskell A, Jandova A, Kimura MT, Carton Y (2021) DROP: Molecular voucher database for identification of *Drosophila* parasitoids. Molecular Ecology Resources 21: 2437–2454. https://doi.org/10.1111/1755-0998.13435

Lohse K (2009) Can mtDNA barcodes be used to delimit species: A response to Pons et al. (2006). Systematic Biology 58: 439–442. https://doi.org/10.1093/sysbio/syp039

Masters BC, Fan V, Ross HA (2011) Species Delimitation – a Geneious plugin for the exploration of species boundaries. Molecular Ecology Resources 11: 154–157. https://doi.org/10.1111/j.1755-0998.2010.02896.x

Minh BQ, Schmidt HA, Chernomor O, Schrempf D, Woodhams MD, von Haeseler A, Lanfear R (2020) IQ-TREE 2: New Models and Efficient Methods for Phylogenetic Inference in the Genomic Era. Molecular Biology And Evolution 37: 1530–1534. https://doi.org/10.1093/molbev/msaa015

Naser-Khdour S, Minh BQ, Zhang W, Stone EA, Lanfear R. (2019) The prevalence and impact of model violations in phylogenetic analysis. Genome Biology and Evolution 11: 3341–3352. https://doi.org/10.1093/gbe/evz193

Nomano FY, Kasuya N, Matsuura A, Suwito A, Mitsui H, Buffington ML, Kimura MT (2017) Genetic differentiation of *Ganaspis brasiliensis* (Hymenoptera: Figitidae) from East and Southeast Asia. Applied Entomology and Zoology 52: 429–437. https://doi.org/10.1007/s13355-017-0493-0

Nurk S, Bankevich A, Antipov D, Gurevich AA, Korobeynikov A, Lapidus A, Prjibelski AD, Pyshkin A, Sirotkin A, Sirotkin Y, Stepanauskas R, Clingenpeel SR, Woyke T, McLean JS, Lasken R, Tesler G, Alekseyev MA, Pevzner PA (2013) Assembling single-cell genomes and mini-metagenomes from chimeric MDA products. Journal of Computational Biology 20(10): 714–737. https://doi.org/10.1089/cmb.2013.0084

Prebus MM (2021) Phylogenomic species delimitation in the ants of the *Temnothorax salvini* group (Hymenoptera: Formicidae): an integrative approach. Systematic Entomology 46: 307–326. https://doi.org/10.1111/syen.12463

Rosen D (1986) The role of taxonomy in effective biological control programs. Agriculture, Ecosystems and Environment 15: 121–129. https://doi.org/10.1016/0167-8809(86)90085-X

Schär ST, Rana G, Espadaler J, Cover X, Shattuck S, Roger S (2022) Integrative taxonomy reveals cryptic diversity in North American *Lasius* ants, and an overlooked introduced species. Scientific Reports 12: 5970. https://doi.org/10.1038/s41598-022-10047-9

Seehausen ML, Ris N, Driss L, Racca A, Girod P, Warot S, Borowiec N, Toševski I, Kenis M (2020) Evidence for a cryptic parasitoid species reveals its suitability as a biological control agent. Scientific Reports 10: 19096. https://doi.org/10.1038/s41598-020-76180-5

Ströher PR, Zarza E, Tsai W, McCormack J, Feitosa R, Pie M (2017) The mitochondrial genome of *Octostruma stenognatha* and its phylogenetic implications. Insectes Society 64: 149–154. https://doi.org/10.1007/s00040-016-0525-8

Struck TH, Feder JL, Bendiksby M, Birkeland S, Cerca J, Gusarov VI, Kistenich S, Larsson KH, Liow LH, Nowak MD, Stedje B, Bachmann L, Dimitrov D (2018) Finding Evolu-

tionary Processes Hidden in Cryptic Species. Trends Ecolology and Evolution 33:153–163. https://doi.org/10.1016/j.tree.2017.11.007

Tagliacollo VA, Lanfear R (2018) Estimating improved partitioning schemes for ultraconserved elements. Molecular Biology and Evolution 35: 1798–1811. https://doi.org/10.1093/molbev/msy069

Talavera G, Castresana J (2007) Improvement of phylogenies after removing divergent and ambiguously aligned blocks from protein sequence alignments. Systematic Biology 56: 564–577. https://doi.org/10.1080/10635150701472164

van Lenteren JC, Isidoro N, Bin F (1998) Functional anatomy of the ovipositor clip in the parasitoid *Leptopilina heterotoma* (Thompson) (Hymenoptera: Eucoilidae), a structure to grip escaping larvae. International Journal of Insect Morphology and Embryology 27: 263–268. https://doi.org/10.1016/S0020-7322(98)00019-1

van Noort S, Buffington ML, Forshage M (2015) Afrotropical Cynipoidea (Hymenoptera). ZooKeys 493: 1–176. https://doi.org/10.3897/zookeys.493.6353

Wang Y, Zhou QS, Qiao HJ, Zhang AB, Yu F, Wang X, Zhu CD, Zhang YZ (2016) Formal nomenclature and description of cryptic species of the *Encyrtus sasakii* complex (Hymenoptera: Encyrtidae). Scientific Reports 6: 34372. https://doi.org/10.1038/srep34372

Zhang YM, Sheikh SI, Ward AKG, Forbes AA, Prior KM, Stone GM, Gates MW, Egan SP, Zhang L, Davis C, Weinersmith KL, Melika G, Lucky A (2022) Delimiting the cryptic diversity and host preferences of *Sycophila* parasitoid wasps associated with oak galls using phylogenomic data. Molecular Ecology 31: 4417–4433. https://doi.org/10.1111/mec.16582

Supplementary material 1

Supplementary data

Authors: Jeffrey Sosa-Calvo, Mattias Forshage, Matthew L. Buffington

Data type: xlsx

Explanation note: **table S1.** Voucher specimen data (FIMS) and SRA accession numbers for the *Ganaspis* samples used in this study; **table S2.** Assembly statistics for all the samples included in this study; **table S3.** SPRUCEUP manual cut-off employed in this study; **table S4.** Alignment statistics and summary of alignments and partitions generated in this study; **table S5.** Summaries of *intra* and *inter* tree distances for the three major clades identified in this study: *Ganaspis brasiliensis*, *G. lupini* sp.nov., and *G. kimorum* sp. nov.; **table S6.** Voucher specimen data and GenBank accession number for the *Ganaspis* samples for which COI sequences were generated.

Link: https://doi.org/10.3897/jhr.97.118567.suppl1